

STUDY OF ^{20}Ne INDUCED REACTION IN ^{59}Co: INCOMPLETE AND COMPLETE FUSION

BY

NTUMBA LOBO

A THESIS SUBMITTED TO THE SCHOOL OF GRADUATE STUDIES OF ADDIS ABABA UNIVERSITY IN PARTIAL FULFILLMENT OF THE REQUIREMENTS FOR THE DEGREE OF MASTER OF SCIENCE IN PHYSICS

AT

ADDIS ABABA UNIVERSITY

ADDIS ABABA, ETHIOPIA

JUNE, 2016

Copy right by NTUMBA LOBO, 2016

ADDIS ABABA UNIVERSITY

DEPARTMENT OF

PHYSICS

Advisor: _____

Prof.A.K. Chaubey

Examiner: _____

Examiner: _____

ADDIS ABABA UNIVERSITY

Date: JUNE 2016

Author**:** **NTUMBA LOBO**

Title**:** **STUDY OF ^{20}Ne INDUCED REACTION IN ^{59}Co: INCOMPLETE AND COMPLETE FUSION**

Department: **Physics**

Degree: **M.Sc** Convocation: **JUNE** Year: **2016**

Permission is herewith granted to Addis Ababa University to circulate and to have copied for non-commercial purposes, at its discretion, the above title upon the request of individuals or institutions.

_____

Signature of Author

THE AUTHOR DOES NOT RESERVE OTHER PUBLICATION RIGHTS, AND NEITHER THE THESIS NOR EXTENSIVE EXTRACTS FROM IT MAY BE PRINTED OR OTHERWISE REPRODUCED WITHOUT THE AUTHOR'S WRITTEN PERMISSION.

THE AUTHOR ATTESTS THAT PERMISSION HAS BEEN OBTAINED FOR THE USE OF ANY COPYRIGHTED MATERIAL APPEARING IN THIS THESIS (OTHER THAN BRIEF EXCERPTS REQUIRING ONLY PROPER ACKNOWLEDGMENT IN SCHOLARLY WRITING) AND THAT ALL SUCH USE IS CLEARLY ACKNOWLEDGED.

TABLE OF CONTENTS

LIST OF TABLES 6

LIST OF FIGURES 7

ABSTRACT 8

ACKNOWLEDGMENTS 9

I.INTRODUCTION 10

II.NUCLEAR REACTION THEORIES 12

2.1 TYPES OF NUCLEAR REACTIONS 14

2.2. Reaction Mechanisms 17

2.2.1 Direct Reactions 18

2.2.2 Compound Nucleus Reactions 20

2.2.3 Pre-equilibrium Reaction 23

2.3 Reaction Cross-section 24

2.4 Heavy Ion Reactions 26

2.4.1 Complete Fusion of HI 29

2.4.2 Incomplete Fusion of HI 30

2.5 Nuclear Reactions and Models 31

2.5.1 Intra-nuclear Cascade Model (INC) 31

2.5.2 Harp-Miller-Berne Model 32

2.5.3 The Exciton Model 32

2.5.4 The Hybrid Model 35

2.5.5 Geometry Dependent Hybrid Model 35

III. EXPERIMENTAL DETAILS 36

3.1 Experimental Method 36

3.2 Sample preparation 37

3.3 Experimental Errors 37

IV.THE COMPUTER CODES AND FORMULATION 38

4.1 Analysis with Computer Codes 38

4.1 .1 PACE4 38

4.1.2 COMPLET 40

V. RESULT AND DISCUSSION 45

V.1. Production of Residues 46

V.1.1.The production of Krypton 46

V.1.2.The production of Bromine 49

V.1.3.The production of selenium 53
V.1.4.The production of Arsenic 55
V.1.5.The production of GERMANIUM 58
V.1.6.The production of GALLIUM 59
V.1.7.The production of COPPER 63
VI. CONCLUSION 65
REFERENCES 66

LIST OF TABLES

TAB4- 1: Theoreticaland measured cross-section for the reaction $^{59}_{27}\mathrm{Co}(^{20}_{10}\mathrm{Ne}, \mathrm{Pn})^{77}_{36}\mathrm{Kr}$used for studyingthe effect of the value of “k” on theoretically calculated results 39
TAB4- 2: Theoretical and measured cross-section for the reaction $^{59}_{27}\mathrm{Co}(^{20}_{10}\mathrm{Ne}, \alpha)^{75}_{35}\mathrm{Br}$used for studying theeffect of exciton number n0 on theoretically calculated results 41
TAB4- 3: Theoretical and measured cross-section for the reaction $^{59}_{27}\mathrm{Co}(^{20}_{10}\mathrm{Ne}, \alpha)^{75}_{35}\mathrm{Br}$used for studying the effect of cmfp parameter on theoretically calculated results 42
TAB4- 4: Theoretical And Measured Cross-Section For The Reaction $^{59}_{27}\mathrm{Co}(^{20}_{10}\mathrm{Ne}, \alpha)^{75}_{35}\mathrm{Br}$used for studying the effect of the value of “k” on theoretically calculated results 43
TAB5- 1: Theoretical And Measured Cross-Section For The Reaction $^{59}_{27}\mathrm{Co}(^{20}_{10}\mathrm{Ne}, \mathrm{pn})^{77}_{36}\mathrm{Kr}$..... 46
TAB5- 2: Theoretical And Measured Cross-Section For The Reaction $^{59}_{27}\mathrm{Co}(^{20}_{10}\mathrm{Ne}, \mathrm{p2n})^{76}_{36}\mathrm{Kr}$ 47
TAB5- 3: Theoretical And Measured Cross-Section For The Reaction $^{59}_{27}\mathrm{Co}(^{20}_{10}\mathrm{Ne}, 2\mathrm{pn})^{76}_{35}\mathrm{Br}$ 49
TAB5- 4: Theoretical And Measured Cross-Section For The Reaction $^{59}_{27}\mathrm{Co}(^{20}_{10}\mathrm{Ne}, \alpha)^{75}_{35}\mathrm{Br}$..... 51
TAB5- 5: Theoretical And Measured Cross-Section For The Reaction $^{59}_{27}\mathrm{Co}(^{20}_{10}\mathrm{Ne}, \alpha 2\mathrm{n})^{74}_{35}\mathrm{Br}$ 52
TAB5- 6: Theoretical And Measured Cross-Section For The Reaction $^{59}_{27}\mathrm{Co}(^{20}_{10}\mathrm{Ne}, \alpha\mathrm{pn})^{73}_{34}\mathrm{Se}$ 53
TAB5- 7: Theoretical AndMeasured Cross-Section For The Reaction $^{59}_{27}\mathrm{Co}(^{20}_{10}\mathrm{Ne}, 4\mathrm{n}\alpha\mathrm{p})^{70}_{34}\mathrm{Se}$ 54
TAB5- 8: Theoretical And Measured Cross-Section For The Reaction $^{59}_{27}\mathrm{Co}(^{20}_{10}\mathrm{Ne}, 2\mathrm{pn}\alpha)^{72}_{33}\mathrm{As}$ 55
TAB5- 9: TheoreticalAnd MeasuredCross-Section For The Reaction $^{59}_{27}\mathrm{Co}(^{20}_{10}\mathrm{Ne}, 2\alpha)^{71}_{33}\mathrm{As}$ 56
TAB5- 10: Theoretical And Measured Cross-Section For The Reaction $^{59}_{27}\mathrm{Co}(^{20}_{10}\mathrm{Ne}, 2\alpha\mathrm{n})^{70}_{33}\mathrm{As}$ 57
TAB5- 11: Theoretical And Measured Cross-Section For The Reaction $^{59}_{27}\mathrm{Co}(^{20}_{10}\mathrm{Ne}, 2\alpha\mathrm{pn})^{69}_{32}\mathrm{Ge}$..... 58
TAB5- 12: Theoretical And Measured Cross-Section For The Reaction $^{59}_{27}\mathrm{Co}(^{20}_{10}\mathrm{Ne}, 3\alpha)^{67}_{31}\mathrm{Ga}$ 59
TAB5- 13: Theoretical And Measured Cross-Section For The Reaction $^{59}_{27}\mathrm{Co}(^{20}_{10}\mathrm{Ne}, 3\alpha\mathrm{n})^{66}_{31}\mathrm{Ga}$ 61
TAB5- 14: Theoretical And Measured Cross-Section For The Reaction $^{59}_{27}\mathrm{Co}(^{20}_{10}\mathrm{Ne}, 4\alpha 2\mathrm{n})^{67}_{31}\mathrm{Cu}$..... 63

LIST OF FIGURES

FIG2- 1: Shows Overview Of Reaction Mechanisms 18
FIG2- 2: Neutron Emission Spectrum Showing Contributions Of Different Reaction Mechanisms In Nuclear Reaction 18
FIG2- 3: Diagramme Representation Of Heavy Ion Reaction 27
FIG4- 1: Excitation Function For The Reaction $^{59}_{27}Co(^{20}_{10}Ne, pn)^{77}_{36}Kr$Used For Studying The Effect Of The Value Of "K" On Theoretically Calculated Results 40
FIG4- 2: Excitation Function For The Reaction $^{59}_{27}Co(^{20}_{10}Ne, \alpha)^{75}_{35}Br$ Used For Studying The Effect Of Exciton Number N_o On Theoretically Calculated Results 42
FIG4- 3: Excitation Function For The Reaction $^{59}_{27}Co(^{20}_{10}Ne, \alpha)^{75}_{35}Br$Used For Studying The Effect Of Cmfp Parameter On Theoretically Calculated Results 43
FIG4- 4: Excitation Function For The Reaction $^{59}_{27}Co(^{20}_{10}Ne, \alpha)^{75}_{35}Br$Used For Studying The Effect Of The Value Of "K" On Theoretically Calculated Results 44

FIG5- 1: The Production Of Krypton $^{59}_{27}Co(^{20}_{10}Ne, pn)^{77}_{36}Kr$ 46
FIG5- 2: The Production Of Krypton $^{59}_{27}Co(^{20}_{10}Ne, p2n)^{76}_{36}Kr$ 47
FIG5- 3: The Production Of Bromine $^{59}_{27}Co(^{20}_{10}Ne, 2pn)^{76}_{35}Br$ 49
FIG5- 4: Production Of Bromine $^{59}_{27}Co(^{20}_{10}Ne, \alpha)^{75}_{35}Br$ 51
FIG5- 5: The Production Of Bromine $^{59}_{27}Co(^{20}_{10}Ne, \alpha 2n)^{74}_{35}Br$ 52
FIG5- 6: The Production Of Selenium $^{59}_{27}Co(^{20}_{10}Ne, \alpha pn)^{73}_{34}Se$ 53
FIG5- 7: The Production Of Selenium $^{59}_{27}Co(^{20}_{10}Ne, \alpha p4n)^{70}_{34}Se$ 54
FIG5- 8: The Production Of Arsenic $^{59}_{27}Co(^{20}_{10}Ne, \alpha 2pn)^{72}_{33}As$ 55
FIG5- 9: The Production Of Arsenic $^{59}_{27}Co(^{20}_{10}Ne, 2\alpha)^{71}_{33}As$ 56
FIG5- 10: The Production Of Arsenic $^{59}_{27}Co(^{20}_{10}Ne, 2\alpha n)^{70}_{33}As$ 57
FIG5- 11: The Production Of Germanium $^{59}_{27}Co(^{20}_{10}Ne, 2\alpha pn)^{69}_{32}Ge$ 58
FIG5- 12: The Production Of Gallium $^{59}_{27}Co(^{20}_{10}Ne, 3\alpha)^{67}_{31}Ga$ 59
FIG5- 13: The Production Of Gallium $^{59}_{27}Co(^{20}_{10}Ne, 3\alpha n)^{66}_{31}Ga$ 61
FIG5- 14: The Production Of Copper $^{59}_{27}Co(^{20}_{10}Ne, 4\alpha 2n)^{67}_{31}Cu$ 63

ABSTRACT

The excitation functions for several residues produced in the system $^{20}Ne+^{59}Co$ have been studied in the energies range 62.9-150.2 MeV. The experimental excitation functions have been compared with those calculated using computer code PACE4 and COMPLET.

The experimental studied production cross-sections for non-alpha emitting channels were found to be in good agreement with theoretical predictions which may be attributed to the complete fusion (CF) processes. However in case of alpha emitting channels, there are signatures of incomplete fusion for more than two alphas emitting and pre-equilibrium for alpha emitting reactions.

ACKNOWLEDGMENTS

Though only my name appears on the cover of this dissertation, a great many people have contributed to its production. I owe my gratitude to all those people who have made this dissertation possible and because of whom my master experience has been one that I will cherish forever.

My deepest gratitude is to my advisor, Prof. A. K. Chaubey. I have been amazingly fortunate to have an advisor who gave me the freedom to explore on my own and at the same time the guidance to recover when my steps faltered. Don taught me how to question thoughts and express ideas. His patience and support helped me overcome many crisis situations and finish this dissertation. I hope that one day I would become as good an advisor to my students as Don has been to me.

I am also thankful to Addis Ababa University (Department of Physics) provided and for extending facilities for carrying out this thesis.

I am indebted to AFIMEGQ scholarship for the financial support provided and for extending facilities for carrying out this thesis.

Finally, most importantly, none of this would have been possible without the love and patience of my family. My immediate family, to whom this dissertation is dedicated to, has been a constant source of love, concern, support and strength all these years. I would like to express my heart-felt gratitude to my family. My extended family has aided and encouraged me throughout this endeavour.

I.INTRODUCTION

Now days the study of the interaction of heavy ions is atopic which has acquired a central place in nuclear physics research [1, 2]. This is possible with the availability of the accelerated beams of heavy ions. Recent studies show that there are different reaction mechanisms in heavy ion reactions at energies around the coulomb barrier to well above it. These reaction mechanisms have been discussed in recent papers [2, 3].

The formation of compound nucleus [1, 2] is the dominant process at lower excitation energies. In compound nucleus formation reactions, the projectile is captured by the target nucleus and its energy is shared and re-shared among the nucleons of the compound nucleus until it reaches a state of statistical equilibrium. After a time much longer than the time required by the projectile to cross the nucleus, a nucleon or a group of nucleons near the surface may, by a statistical fluctuation, receive enough energy to escape, just as a molecule may evaporate from a heated drop of liquid.

At moderate excitation energies [1, 2], however, there are indications that pre-equilibrium emission (where there is emission of a particle long before the attainment of statistical equilibrium) also contributes to the reaction processes.

Late experimental [2, 3] studies have shown that complete fusion and incomplete fusion reactions play important roles in heavy ion reactions. In the complete fusion reaction process [1, 2], the projectile completely fuses with the target nucleus. In this case, the entire momentum of the projectile is transferred to the target nucleus. In the case of incomplete fusion reaction [1, 2], only a part of the incident ion fuses with the target and the remaining part moves in the direction of the incident beam with almost the same velocity. In this case, the fraction of the momentum transferred depends on the mass of the fused fragment.

The main objective of this study is to study complete and incomplete reaction mechanisms in the light (medium) target nucleus. This is accomplished by the study of the excitation functions of the residues produced in the system ^{20}**Ne+**^{59}**Co**.

This and other measurements [4] have shown the importance of complete and incomplete fusion as well as of pre-equilibrium emission processes in heavy ion reactions at energies around the coulomb barrier. The excitation functions for eight reactions produced in the **^{20}Ne+^{59}Co** system have been measured [5] in the energy range ≈62.9-150.2 MeV to study complete fusion and incomplete fusion reactions in heavy ion reactions. Recently, it has been observed that the incomplete fusion becomes more and more dominant as the projectile energy increases.

The present experimental values [5] are taken from experiments done using theInter-University Accelerator Centre, New Delhi, India, where data are found in EXFOR web site. The measured excitation functions are compared with theoretical calculations obtained using the computer programs PACE4[2] and, COMPLET[6] which evaluates the cross-sections for evaporation residues formed in the complete fusion reaction process of the projectile with the target without taking the incomplete fusion reaction process into account.

II.NUCLEAR REACTION THEORIES

In 1932, the English physicist John Cockcroft and the Irish physicist Ernest Walton [13] produced a nuclear disintegration by bombarding Lithium with artificially accelerated protons. The following reaction took place:

$$^{7}_{3}\mathbf{Li} + ^{1}_{1}\mathbf{H} \rightarrow ^{4}_{2}\mathbf{He} + ^{4}_{2}\mathbf{He} + \mathbf{Energy.}$$

This was the first artificial splitting of a nucleus. It was also the first transmutation using artificially accelerated particles. Protons were accelerated and slammed into lithium atoms producing alpha-particles and energy. Thus the mass of the proton and lithium was converted into the mass of two alpha-particles and kinetic energy. This reaction was the first experimental proof of Einstein's $\mathbf{E=mc^2}$. Cockcroft and Walton won a Nobel Prize in physics in **1951**.

In physics, a nuclear reaction [14] is a process in which the structure and energy content of an atomic nucleus are changed by interaction with another nucleus or particle. Basically, a reaction may implicate more than two particles hitting, however the probability of three or more nuclei to encounter at the same moment and same locus is plenty less than two nuclei, such an occurrence is extremely uncommon.

The study of nuclear reactions is one substantial field of scrutiny to comprehend nuclear reaction mechanism and other nuclear structure properties. Most of the known nuclear reaction is produced by exhibiting dissimilar materials to a beam of accelerated particles.

The energy must be high enough to surmount the natural repulsion between the ion and nuclear protons. This energy barrier is called the Coulomb barrier. If the energy is below the barrier, the reaction will bounce off each other.

Studying nuclear reactions [14] is important for a number of reasons. Progress in the understanding of nuclear reactions has occurred at a faster pace and generally a higher level of sophistication has been achieved compared to similar studies of chemical reactions. The approaches used to understand nuclear reactions are of value to any chemist who wishes a deeper insight into chemical reactions. There are certain nuclear reactions that play a preeminent role in the affairs of man and our understanding of the natural

world in which we live. For example, life on earth would not be possible without the energy provided to us by the sun. That energy is the energy released in the nuclear reactions that drive the sun and other stars. For better or worse, the nuclear reactions, fission and fusion, are the basis for nuclear weapons, which have shaped much of the geopolitical dialog for the last 50 years. Apart from the intrinsically interesting nature of these dynamic processes, their practical importance would be enough to justify their study. To discuss nuclear reactions effectively we must understand the notation or jargon that is widely used to describe them. Let us begin by considering the nuclear reaction: $^{4}\mathbf{He}+^{14}\mathbf{N}\rightarrow^{17}\mathbf{O}+^{1}\mathbf{H}$.

Most nuclear reactions [13] are studied by inducing a collision between two nuclei where one of the reacting nuclei is at rest (the target nucleus) while the other nucleus (the projectile nucleus) is in motion. (Exceptions to this occur both in nature and in the laboratory in studies where both the colliding nuclei are in motion relative to one another). But let us stick to the scenario of a moving projectile and a stationary target nucleus. Such nuclear reactions can be described generically as

(Projectile)**P+(target)T→(residual nucleus) R+ (emitted particle) X**.

For example, the first reaction discussed above might occur by bombarding $^{14}\mathbf{N}$ with alpha particles to generate an emitted particle, the proton and a residual nucleus$^{17}\mathbf{O}$.A shorthand way to denote such reactions is, for the general case, **T(P, x) R** or for the specific example $^{14}\mathbf{N}(\alpha, p)^{17}\mathbf{O}$.

In a nuclear reaction [1, 8] , there is conservation of the number of protons and neutrons (and thus the number of nucleons). Thus the total number of neutrons (protons) on the left and right sides of the equations must be equal. There is also conservation of energy, momentum, angular momentum and parity .

2.1 TYPES OF NUCLEAR REACTIONS

There are different types of nuclear reactions [8].

ELASTIC COLLISIONS

The interaction in which the system remains in its initial quantum mechanical parameters (Initial state); in this interaction there is no appreciable transfer of energy [no appreciable energy loss]. In these interactions, system remains in the ground state. This system is not excited.

(Projectile) x+ (target) X→ X (residual) +x (outgoing particle)

$$^{4}_{2}\mathbf{He} + \ ^{197}_{79}\mathbf{Au} \rightarrow \ ^{197}_{79}\mathbf{Au} + \ ^{4}_{2}\mathbf{He}$$

INELASTIC COLLISIONS

a) Excitation

Consider the previous statement the emitted particle remains same but with lower energy and the target nucleus X is X^*in excited state.

x + X $\cancel{X^*}$ → x'

For example:

$^{1}_{1}\mathbf{H} + \ ^{7}_{3}\mathbf{Li} \rightarrow \ ^{7}_{3}\mathbf{Li}^* + \ ^{1}_{1}\mathbf{H}$(Lower energy)→ $^{7}_{3}\mathbf{Li} + \ ^{1}_{1}\mathbf{H} + \boldsymbol{\gamma}$

b) Radiative Capture of Projectile

In this inelastic collision the projectile (incident particle) is captured by target nucleus and a new system is formed. Onlyγ-radiation is emitted and no other particle is emitted.

$^{1}_{1}\mathbf{H} + \ ^{26}_{12}\mathbf{Mg} \rightarrow \left(^{27}_{13}\mathbf{Al}\right)^* \rightarrow \ ^{27}_{13}\mathbf{Al} + \boldsymbol{\gamma}$

γ- Rays emitted are high energy photon called promptγ, because these are emitted promptly (immediately)

c) Disintegration Process

The projectile is captured by target nucleus. The system formed disintegrates into a new residual nucleus while one or more particles are emitted. That is,**(Projectile) x+ (target) X → C (C= x + X) → Y (residual system) +y (emitted particle)**

We can write in the short form as: **x (X, Y) y**

Disintegration depends upon the projectile energy or the excitation energy of compound nucleus.

$x + X \rightarrow C \rightarrow Y_1 + y_1$ or

$x + X \rightarrow C \rightarrow Y_2 + y_2$ or

$x + X \rightarrow C \rightarrow Y_3 + y_3$

The emitted particles $y_1, y_2, y_3, \ldots$ can be one or more particles. This also follows **ϒ-**Ray emission.

$$_{2}^{4}\mathbf{He} + {}_{7}^{14}\mathbf{N} \rightarrow {}_{9}^{18}\mathbf{F} \rightarrow {}_{8}^{17}\mathbf{O} + {}_{1}^{1}\mathbf{H}$$

d)Many Body Interactions

Many particles may be emitted depending upon the excitation energy of compound nucleus.

^{16}O (P, 2P) ^{15}N

^{16}O (P, Pn) ^{15}O

^{16}O (P, 3P) ^{14}C etc...

e)Photo-Disintegration

The reactions induced by ϒ-rays, at high energy may have photo-disintegration

i.e. $\mathbf{\Upsilon + {}_{1}^{2}H \rightarrow {}_{1}^{1}H + {}_{0}^{1}n}$ Photo-disintegration of deuteron. For such reaction ϒ-ray energy should be higher than threshold energy.

f)Stripping and Pick-up Reactions

These are interaction in which projectile interacts with few surface nucleons. If the projectile is combination of nucleons, it may be stripped off one or more which absorbed and remaining part of the projectile is emitted.

$_{1}^{2}\mathbf{H} + {}_{29}^{63}\mathbf{Cu} \rightarrow {}_{29}^{64}\mathbf{Cu} + {}_{1}^{1}\mathbf{H}$ (stripping reaction)

Opposite of this is pickup, in which the projectile pick up a nucleon from target a composite system is emitted.

$_{1}^{1}\mathbf{H} + {}_{13}^{27}\mathbf{Al} \rightarrow {}_{13}^{26}\mathbf{Al} + {}_{1}^{2}\mathbf{H}$ (pickup reaction)

Stripping and Pick-up Reactions are also called direct reaction. These take place at high energy of projectile.

HEAVY IONS REACTIONS

These reactions are induced by heavy ions; they can be compound nucleus reactions and direct reactions.

$^{14}N + {}^{207}Pb \rightarrow {}^{13}N + {}^{208}Pb$

ELEMENTARY PARTICLE REACTIONS

Means reaction induced by elementary particles in which production of mesons (pion, heavy, and meson) takes place .So these are also at the high energy of projectile.

$p+p \rightarrow p+n+\pi^{+}$

$\pi^{-}+p \rightarrow \pi^{0} + n$

$p +\pi^{0} \rightarrow K^{+} +\Lambda^{0}$

NUCLEAR FISSION AND FUSIONS REACTIONS

The interaction in which, heavy nucleus splits into two medium nuclei is called nuclear fission reactions.

$^{235}_{92}U + {}^{1}_{0}n \rightarrow {}^{98}_{40}Zr + {}^{136}_{52}Te + 2\ {}^{1}_{0}n$ + **Energy** **(**nuclear fission**)**

In fusion reaction there is a combination of two nuclei to form a more massive nucleus.

$^{2}D + {}^{3}T \rightarrow {}^{4}H + \gamma$

2.2. Reaction Mechanisms

In nuclear reaction, there are three mechanisms of nuclear reaction [13]. These are direct reaction, compound nucleus reaction and pre-equilibrium reaction. The direct reaction takes place in the time the projectile takes to traverse the target nucleus (~10^{-22}s). In this reaction, the projectile may interact with a nucleon, a group of nucleons or with the whole nucleus and emission takes place immediately.

The compound nucleus reaction takes place when the projectile is captured by the target nucleus. In this reaction, the energy and momentum of the projectile is shared and re-shared among the nucleons of the compound nucleus until it reaches a state of statistical equilibrium. This transfer of energy and momentum takes so much time (~10^{-15}s) that the incoming projectile becomes part of the system because there is a thorough mixing of all the nucleons energy.

The pre-equilibrium reaction is a reaction mechanism where a particle is emitted neither immediately after the interaction of the projectile with a nucleon or with a group of nucleons of the target nucleus, as in a direct reaction, nor after a long time by the statistical decay of the compound nucleus. The projectile may share its energy among a small number of nucleons which may further interact with other nucleons, and this cascade of nucleon-nucleon interactions through which the energy of the incident particle is progressively shared among the target nucleons, a particle may be emitted long before the attainment of statistical equilibrium.

All these reactions are subject to the conservation laws of energy, momentum, mass number, spin, total charge, parity, lepton number, baryon number, etc. The relative importance of these three reaction mechanisms depends on the type of interacting particles and their relative energy.

In these different types of reaction mechanisms, after the first interactions, the nucleon may leave the nucleus immediately by a direct reaction or it may interact with a nucleon in the nucleus and start a cascade of nucleon-nucleon interaction from which pre-equilibrium emission may occur. During this cascade, the energy is shared among an increasing number of nucleons until eventually the compound nucleus is formed. The compound nucleus may decay into the elastic or any of the reaction channels that are allowed energetically. The shape elastic and compound elastic processes combine to give the measured elastic scattering cross-section. In a similar way the direct, pre-equilibrium and compound nucleus processes combine to give the inelastic cross-sections and all the other non-elastic reactions. This shows the connection between the different reaction mechanisms**.**

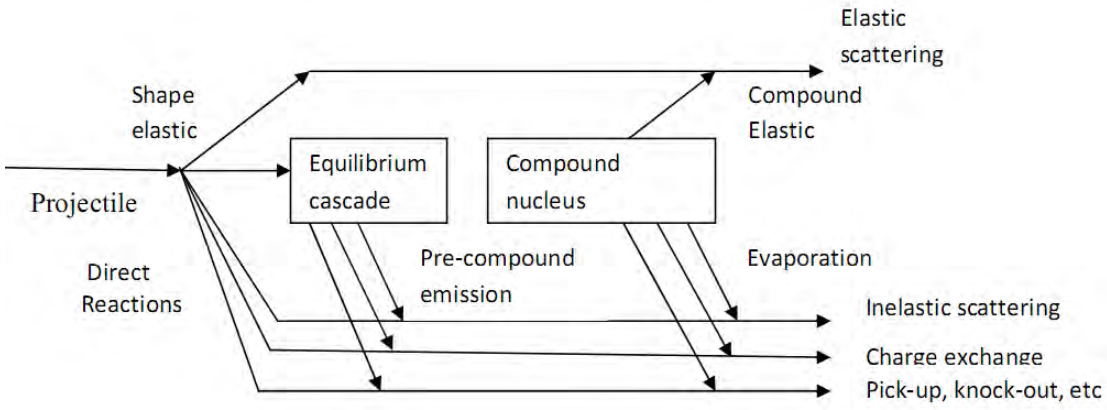

FIG2- 1: Shows overview of reaction mechanisms [13]

All the above mentioned reaction mechanisms may contribute to a given reaction and an experiment may focus on one contribution or the other. To show this, consider the elastic scattering of a nucleon or a proton by a nucleus. At low energies, neutrons and protons interact very differently. Protons are repelled by the electrostatic field of the nucleus and are scattered elastically with a cross-section given by Rutherford's formula. This is a direct reaction. Low energy neutrons may be scattered by the nuclear field (this is potential scattering, or shape elastic scattering, a direct process) or may be captured to form the compound nucleus and then emitted with the same energy. This is compound elastic scattering, which is strongly affected by the structure of the compound nucleus.

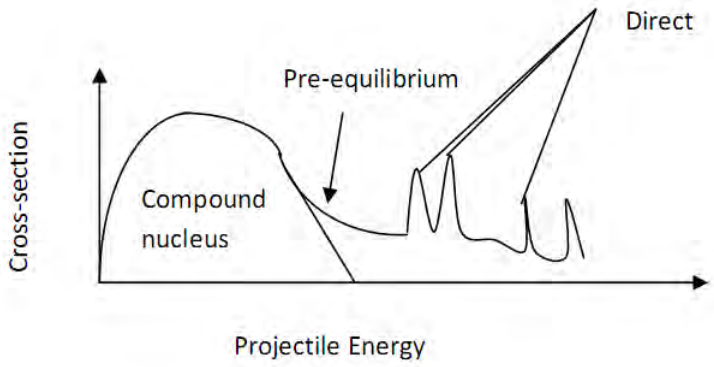

FIG2- 2: Neutron emission spectrum showing contributions of different reaction mechanisms in nuclear reaction [13]

2.2.1 Direct Reactions

A direct reaction [1] occurs when the projectile interacts primarily with the nucleons in the surface of the target nucleus. The interaction is with one or two nucleons. Energy and momentum transfer is very small and the transfer is to only few

nucleons, and emission of the particle most probably is in the direction of motion of the projectile.

The main characteristics of direct reactions are: first the emission of much larger number of high energy particles than expected on the basis of evaporation model. Second, the angular distribution of emitted particles shows a forward peaking. This is may be because the direct reaction takes place with surface nucleons. The third main characteristic of direct reaction is a monotonic change of cross-section with energy, no resonances are observed. Direct reactions take place, generally, at higher energies.

There are a number of reactions categorized under the direct reaction. The simplest direct reaction is elastic scattering, which leaves the target nucleus in its ground state. Inelastic scattering occurs when a projectile interacts with a target nucleus and gives it some of its energy, raising it to an excited state. Measurement of the loss of energy gives the energy of the excited state.

At low incident energies the target nucleus can be excited purely by the coulomb excitation and is appreciable only for highly charged projectiles-heavy ions. At higher energies the excitation is due to the nuclear interaction between the projectile and target modified by the presence of the coulomb field. By inelastic scattering, mainly, it is collective states that are strongly excited. This shows that the projectile interacts with the target nucleus as a whole, not just with one of its constituent nucleon. This is a collective excitation and may be described as a coherent sum of many individual particle-hole excitations.

Charge-exchange reaction is other type of direct reaction. In this reaction both energy and charge are transferred between the projectile and the target nucleus. Charge-exchange reactions show the importance of isospin in nuclear reactions. These reactions are particularly interesting because only the charge-exchange isospin-dependent terms in the effective interaction contribute to the cross-section. If the reaction goes to the isobaric analogue state of the target nucleus the reaction is particularly simple as only the isospin vectors are flipped. Such reactions are very similar to elastic scattering, and are sometimes referred to as quasi-elastic scattering.

The other reaction under the direct reaction is transfer reaction. In this reaction one or more nucleons are transferred from the projectile to the target-stripping or from the target to the projectile-pick up reactions.

As the energy of the projectile increases, it becomes likely that more than one particle is emitted. The simplest examples are the break-up of a composite projectile into its constituents and the knock-out of a nucleon or group of nucleons from the

target nucleus. At low projectile energies, the break-up is due to the coulomb field of the target nucleus, and as the energy increases the nuclear field also contributes. Coulomb break-up is more pronounced for heavy target nuclei. Break-up reactions can have the target in its ground state, or raise it to an excited state; these processes referred to as elastic and inelastic break-up. In a knock-out reaction the incident particle is small compared with the inter nucleon separation in the nucleus, and the projectile energy is much higher than the binding energy of the struck nucleus.

2.2.2 Compound Nucleus Reactions

A compound nucleus [1] reaction is an extreme example of a multistep reaction in which the detailed complexity of the successive steps is lost. In compound nucleus reaction a transfer of energy and momentum takes so much time that the compound nucleus formed forgets the history of formation. If the same compound nucleus is formed by different projectile interactions, it cannot remember the mechanism of its formation.

A compound nucleus state is excited, and gives resonances when the energy brought in by the projectile, plus the capture Q-value coincides with energy of one of its states. These states are excited one by one as the energy increases, and each corresponds to resonance.

It is difficult to give a rigorous description of the process of formation of the compound nucleus. It is a good approximation to assume that, in the sequence of nucleon-nucleon interactions, all the states corresponding to the various configurations are excited with equal probability. When eventually the long-lived compound nucleus is created, all the possible states corresponding to a given set of quantum numbers **E, J, M, π,** form the single-particle to the complex many-particle states, are equally likely. The compound nucleus is then in statistical equilibrium since the probability of occurrence of a given configuration is simply proportional to its statistical weight.

In compound nucleus reactions, after a time much longer than the time required by the projectile to cross the nucleus, a nucleon or a group of nucleons near the surface may, by statistical fluctuation, receive enough energy to escape, just as a molecule may evaporate from a heated drop of liquid. This statistical process favours the evaporation of the particles with energy near the smallest possible energy, which in the case of charged particle is the height of the coulomb potential at the nuclear surface, the coulomb barrier. If the excitation energy of the compound nucleus is high enough, several particles may evaporated in sequence and the process continues until the energy of the nucleus is below the threshold for the particle

emission, and then the nucleus emits γ-rays until it reaches the ground state.

The decay of the compound nucleus is independent of the way it is formed. Its decay will depend only on its quantum mechanical parameter-energy of excitation and momentum. Decay of any excited state depends upon the width of decaying state i.e. $\Gamma=\frac{\hbar}{\tau}$, where τ is mean life of decaying state. The decay probability of compound nucleus is given as $G_c(\beta)=\frac{\Gamma_\beta}{\Gamma}$. The probability of formation of compound nucleus by ά-channel is $\sigma_c(\alpha)$ and nuclear reaction (α, β) is given by $\sigma(\alpha, \beta)=\sigma_c(\alpha)\frac{\Gamma_\beta}{\Gamma}$, where α is incoming channel while Γ_β is the decay of outgoing channel.

The Weisskopf-Ewing theory is the best theory for describing compound nucleus reactions. At low incident energies the compound nucleus states are excited individually each produces a resonance in the cross-section that may be described by the Breit-Wigner theory. As the incident energy increases compound nucleus states of higher energy are excited and these are closer together and of increasing width. Eventually they overlap and it is no longer possible to identify the individual resonances. The cross-section then fluctuates.

This fluctuating behaviour is due to the interference of the reaction amplitudes corresponding to the excitation of each of the overlapping states which vanish in the energy average of the cross-section since these amplitudes are complex functions with random modules and phase. The energy average of the cross-sections thus shows weak energy dependence and it is predicable by the theory. To do this, consider a reaction that proceeds from the initial channel c through the compound nucleus to the final channel c'.

The hypothesis of the independence of formation and decay of the compound nucleus then gives for the cross-section $\sigma_{cc'}=\sigma_{CN}(c)\frac{\Gamma_{c'}}{\Gamma}$, where $\sigma_{CN}(c)$ is the cross-section of the compound nucleus and $\Gamma_{c'}$ and Γ are respectively the energy-averaged width for the decay of the compound nucleus in channel c' and the energy-averaged total width.

Using the reciprocity theorem, which relates the cross-section $\sigma_{cc'}$ to the cross-section for the time reversal process **c'c**, we get

$$g_c k_c^2 \sigma_{cc'} = g_{c'} k_{c'}^2 \sigma_{c'c}$$

where $g_c = 2i_c+1$ and $g_{c'} = 2i_{c'}+1$ are the statistical weights of the initial and final channels, i_c and $i_{c'}$ the spin of the projectile and the ejectile, and k_c and $k_{c'}$ their wave numbers. This gives

$g_c k_c^2 \sigma_{CN}(c)\Gamma_{c'}=g_{c'} k_{c'}^2 \sigma_{CN}(c')\Gamma_c$ or equivalently

$$\frac{\Gamma_c}{g_c k_c^2 \sigma_{CN}(c)} = \frac{\Gamma_{c'}}{g_{c'} k_{c'}^2 \sigma_{CN}(c')}$$

Since the channels **c** and c' are chosen arbitrarily, this relation holds for all possible channels. So $\Gamma_c \alpha g_c k_c^2 \sigma_{CN}(c)$ .Since the total width is obtained by summing the $\Gamma_{c'}$s overall open channels $\Gamma=\Sigma_c\Gamma_c$, the cross-section $\sigma_{cc'}$ becomes

$$\sigma_{cc'} = \sigma_{CN}(c) \frac{g_{c'} k_{c'}^2 \sigma_{CN}(c')}{\Sigma c g_c k_c^2 \sigma_{CN}(c)}$$

Ejectiles with energy in the range $\varepsilon_{c'}$ to $\varepsilon_{c'}+d\varepsilon_{c'}$, have the residual nucleus with energy in the range $U_{c'}$ to $U_{c'}+dU_{c'}$, where $U_{c'}=E_{CN}-B_{c'} -\varepsilon_{c'}$, and E_{CN} and $B_{c'}$ are respectively compound nucleus energy and the binding energy of the ejectile in the compound nucleus.

Introducing the density of levels of the nucleus **w ($u_{c'}$)** the above equation becomes

$$\sigma_{cc'} d\varepsilon_{c'} = \sigma_{CN}(c) \frac{g_{c'} k_c^2 \sigma_{CN}(c') w(u_{c'}) du_{c'}}{\sum_c \int_c^{E_c^{max}} g_c k_c^2 \sigma_{CN}(c) w(u_c) du_c}$$

or since $k^2 = 2m\varepsilon$,

$$\sigma_{cc'}(\varepsilon_{c'}) d\varepsilon_{c'} = \sigma_{CN}(c) \frac{(2i_{c'}+1)\mu_{c'} \sigma_{CN}(c') w(u_{c'}) du_{c'}}{\sum_c \int_c^{E_c^{max}} (2i_c+1)\mu_c \sigma_{CN}(c) w(u_c) du_c}$$

Where μ_c the reduced mass of the ejectile c. This is the Weisskopf-Ewing formula for the angle integrated cross-sections.

To a good approximation, the level density **w(u) α exp($\frac{U}{T}$)**, so the ejectile spectrum given by the Weisskopf-Ewing theory is Maxiwellian. It rises rapidly above the threshold energy, attains a maximum and then falls exponentially.

From the detailed balance principle which in addition to the invariance for the reversal leading to the reciprocity theorem implies the existence of a long-lived compound nucleus state. This principle states that two systems a and b, with state densities ρ_a , are in statistical equilibrium when the depletion of the states of the system a by transition to b equals their increase by the time reversal process b→ a.

If $w_{ab} = \frac{\Gamma_{ab}}{\hbar}$ is the decay rate (probability per unit time) for transitions from a to b and $w_{ba} = \frac{\Gamma_{ba}}{\hbar}$ is the decay rate for the reverse process, this equality occurs when

$$\rho_a \Gamma_{ab} = \rho_b \Gamma_{ba} .$$

The Weisskopf-Ewing theory provides a simple way of estimating the energy variation, at low incident energies, of the cross-section of all available final channels in a particular reaction.

2.2.3 Pre-equilibrium Reaction

Pre-equilibrium reaction [1] is neither direct nor compound nucleus reaction. In this types of reactions particles are emitted after the first stage of a nuclear interaction (direct reaction) but long before the attainment of statistical equilibrium (compound nucleus formation). Their time scale is intermediate between the very fast direct reactions and the relatively slow compound nucleus formation.

In pre-equilibrium reactions, the emission of particles from the excited target nucleus is neither by statistical decay of compound nucleus nor by the prompt emission after collision. In these reactions, the projectile shares its energy among a small number of nucleons in the target; the struck nucleons initiate a cascade of reactions with the target, at the course of which a particle can be emitted before the compound nucleus was reached a state of statistical equilibrium.

The energy of the projectile is shared among the nucleons of the target by a cascade of nucleon-nucleon interactions that excites particle-hole state of increasing complexity. A pre-equilibrium reaction corresponds to emission of an unbound particle from one of these particle-hole states when the composite nucleus is not yet equilibrated.

Most pre-equilibrium reactions take place at energies high enough for it to be no longer possible to resolve the individual final state. The cross-sections are those of reactions to a continuum of final states, and the absence of fluctuations in these continuum spectra shows that to a high degree of accuracy one may assume that there are no interference effects so that pre-equilibrium cross-sections can be evaluated by adding incoherently the contributions from each stage of the nucleon-nucleon interaction cascade. The total cross-section for pre-equilibrium emission is then the sum of the cross-sections for emission from each stage of the cascade.

2.3 Reaction Cross-section

Reaction cross-section [7] is the most important quantity in nuclear reaction study. The reaction cross-section is a measure of the probability for a particular reaction to occur. Since interactions in a nuclear reaction take place with individual target nuclei independently of each other, it is useful to refer to the probability of a nuclear reaction to one target nucleus.

To define the reaction cross-section, assume that in a given experiment a thin slab of target material is struck by mono energetic beam consisting of I particles per unit time distributed uniformly over an area A. If nuclear reaction produces N particles per unit time, we can pretend that with each target nucleus there is associated an area σ which is perpendicular to the incident beam such that if the centre of a bombarding particle strikes inside of σ, there is a hit and a reaction is produced; and if the centre of the bombarding particles misses σ, no reaction is produced.

So the quantity σ is defined as cross-section and it gives a measure of the reaction probability per target nucleus. It is a fictitious area, which need not be related to the cross-sectional area **(πR^2)** of the struck nucleus.

It is also possible to describe the reaction probability by the ratio $\frac{N}{I}$, but this quantity depends on the target density as well as its thickness Δx, whereas σ is associated with an individual target nucleus.

The probability that any one bombarding particle has a hit is equal to $\frac{N}{I}$ and is also equal to the projected total cross-section of all target nuclei lying within the area A, as seen along the beam direction, divided by A. If there are n target nuclei per unit volume in the target material, nAΔX, such nuclei are within reach of any bombarding particle in the beam. Each target nucleus has an associated cross-section **σ** so that $\frac{N}{I}=\frac{nA\Delta X\sigma}{A}$,

Using this relation we can define cross-section by writing

$$\sigma = \frac{N}{\left(\frac{I}{A}\right)(nA\Delta X)}$$

The cross-section has a dimension of area and measured in a unit of cm^2 or barn, where

$1barn=10^{-24}\ cm^2$. Experimentally cross-section is measured by the ratio

$$\sigma = \frac{\text{number of reaction particles emitted per unit time}}{(\text{number of beam particles per unit area per unit time})(\text{number of target nuclei within the beam})}$$

The impact parameter is an important parameter in nuclear reactions to take place, as stated earlier, and it has a connection with the reaction cross-section-the probability for nuclear reaction to take place. To see this connection, consider the projectile beam as particle wave. There will be interaction of beam with target, from classical considerations, when the impact parameter of beam is less than the nuclear radius i.e., if **b ≤ R** interaction takes place and if b>R no interaction is taking place.
Angular momentum is given as **pxb** or **pb**. But from quantum mechanics, angular momentum is quantized and is given as **lħ**, where **l=0, 1, 2, ---.** From this relation we can write angular momentum as **pb = lħ** or the impact parameter **b=lħ/p or b=ƛl**. Where **ƛ=ħ/p** is the reduced de Broglie wave length. This clearly shows that the idea of quantization of angular momentum leads to the quantization of impact parameter.

We can imagine particles of beam moving with having different quantized value of impact parameter. One can divide the particles of beam in different zones having different impact parameters. Particles moving in the central zone having l=0 and impact parameter **b≤ƛ**. In the next zone particles of impact parameter of b value **ƛ<b<2ƛ** having **l=1** are moving. In the next zone particles having **l=2** and impact parameter **2ƛ<b<3ƛ** are moving. In this way particles moving in **l^{th}** zone will have impact parameter in between **lƛ** and **(l+1) ƛ**.

Geometrical area of **l^{lh}** zone will be

$\pi[(l+1)ƛ]^2-\pi(lƛ)^2=\pi ƛ^2(2l+l)$

So the reaction cross-section, $\sigma_{r,l}$ is given as

$\sigma_{r,l}= \pi ƛ^2(2l+l)$ or

$\sigma_r=\sum_l \pi ƛ^2(2l+l) = \pi ƛ^2 \sum_{l=0}^{lm}(2l+l)$

$\sigma_r = \pi ƛ^2 \sum_{l=0}^{lm}(2l+l)$

2.4 Heavy Ion Reactions

The study of heavy ions reaction is a subject of growing interest in nuclear physics [1, 9, 10,11].Because of the heavy mass of the incident heavy ion, angular momentum and plenty of energy can be conveyed to the target nucleus and giving rise to a new observable fact as fission , fusion , etc. . All nuclide heavier than alpha, is a heavy ion. At low energy two heavy ions interact only through their coulomb filed, and can scatter elastically or inelastically with coulomb excitation.

Heavy ion reactions can be divided into three main classes:

1) Due to their huge charge, two heavy nuclei feel a strong mutual coulomb repulsion barrier. For an ever so heavy target, it is necessary about five Mev per nucleon. Subsequently the wave length of the projectile is small compared with the dimensions of nuclei so classical and semi-classical methods become useful in the description of the reaction.

2) The projectile carries a large amount of angular momentum and a part of it can be transferred to the target in the reaction. Rotational bands with several dozens of units of angular momentum can be created. As matter of fact, heavy ion reactions are the best suited to feed high spin levels.

3) Direct reactions and formation of compound nucleus are also common process in reactions with heavy ions. But some peculiarities of these are not found in reactions with projectile nucleon. One of these processes can be understood as intermediate between a direct reaction and formation of compound nucleus. Fusion does not occur but projectile and target pass relatively long time under the mutual action of the nuclear forces. Nuclear matter is exchanged between both and there is a strong heating of two nuclei, with a large transfer of kinetic energy to the internal degrees of freedom. These are the deep inelastic collisions. This process depends on the distance d between the projectile and target.

$$\mathbf{d}=\frac{\mathbf{a}}{\mathbf{2}}+\left[\left(\frac{\mathbf{a}}{\mathbf{2}}\right)^{\mathbf{2}}+\mathbf{b}^{\mathbf{2}}\right]^{\frac{\mathbf{1}}{\mathbf{2}}}$$

$\mathbf{a}=\frac{\mathbf{Z_1 Z_2 e^2}}{\mathbf{4\pi\epsilon_0 E}}$ is the distance of closest approach in a head-on collision. If the two ion energy in the centre of masse system $\mathbf{E_{cm}}$ can surmount the coulomb barrier, nuclear reaction can happen and then the associated wavelength which is less than the nuclear dimensions is equal to:

$\lambda = \frac{h}{\sqrt{2ME_{CM}}}$

$r_{min} = \frac{b}{\sqrt{1-\frac{V(r_{min})}{E_{CM}}}}$ is the minimal distance between the two interacting heavy ions and

$V(r_{min})$ is the nuclear potential acting between the two ions.

If $0 \leq r_{min} \leq R_F$, we are in the fusion region, where R_F is radius of fusion

If $R_F \leq r_{min} \leq R_{DIC}$ we are in the deep inelastic incomplete fusion

If $R_{DIC} \leq r_{min} \leq R_N$ we are in the peripheral region

If $r_{min} > R_N$, R_N is the distance above which nuclear interactions are negligible, we are in the coulomb region.

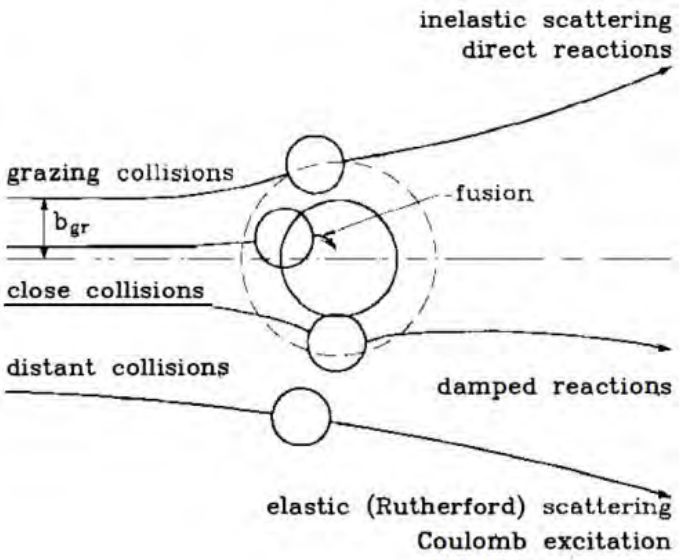

FIG2- 3: Diagramme representation of heavy ion reaction [9]

The ion orbits corresponding to these regions are schematically shown in figure, above in the fusion region the two ion interaction leads predominantly to the formation of composite nucleus which initially is quite far from the statistical equilibrium since a large part of its excitation energy is in the form of an orderly collective translational motion of nucleons of the projectile and the target. This orderly motion is transformed into chaotic thermal motion by means of a cascade of nucleon-nucleon interactions. This thermalization eventually leads to a compound nucleus in statistical equilibrium, but, before reaching this, a considerable fraction of the excitation energy may be carried off fast particles or cluster of particles with

energy considerably greater than the average thermal energy. Nuclear reactions, induced by heavy ions below but near coulomb barrier are useful for exciting the collective model of excitation of the target nuclei. Because coulomb barrier is comparatively high in heavy ion induced reactions and the projectile energies generally available are of the same order as the coulomb barrier, the coulomb barrier energy becomes very good reference energy to describe the reactions.

Finally in the coulomb region the nuclear interaction between the two ions is negligible, but they may still interact via the coulomb excitation. The impact parameter b can be related to the corresponding orbital angular momentum L by the classical relation

$$\mathbf{L\hbar=\mu\nu b=Pb=\hbar kb}$$

Where $\mu$is the two-ion reduced mass, $\nu$and P the two-ion relative velocity and momentum. Previous considerations make it possible to assume, to a first approximation, that the different processes dominate in different L-windows and give approximate expressions for the reaction cross-sections in the different regions as

$$\boldsymbol{\sigma_i=\frac{\pi}{k^2}\sum_{L=L_i}^{L=L_i+1}(2L+1)T_L}$$

The transmission coefficient $\boldsymbol{T_L}$**=1** for **L≤ L_{max}**, and i=1,2,3,4 corresponds ,respectively, to fusion, to deep inelastic or break-up fusion, to peripheral and to coulomb reactions and to coulomb reactions and **L=L_1,L_2,L_3,L_4,L_5** equals, respectively **0,kR_F,kR_{DIC},kR_N,L_{max}**

With $L_{max}=\sqrt{\frac{\sigma^2_{Rint}}{\pi}}-1$

Where$\boldsymbol{\sigma_R}$is the total cross-section including coulomb excitation. The total reaction cross-section to a good approximation is given by the semi-classical expression $\boldsymbol{\sigma_R=\pi R_{int}^2\left[1-\frac{V(R_{int})}{E_{CM}}\right]}$,

Where, the interaction radius R_{int} and the interaction barrier $\mathbf{V(R_{int})}$may be obtained by plotting the product $\boldsymbol{\sigma_R E_{CM}}$($\mathbf{E_{CM}}$ **is** energy in the centre of masse) against the two-ion centre of mass energy.

2.4.1 Complete Fusion of HI

Heavy ion complete fusion reaction [1, 2, 3, 9] is a reaction where there is an entire momentum transfer from projectile to the target nucleus takes place. In this reaction, a fully equilibrated excited compound nucleus of pre-determined charge, mass and angular momentum is formed. Heavy ion fusion reactions have been extensively studied because they offer possibility of producing nuclei with high excitation energy and high spin thus allowing study of nuclear matter in conditions which are not easily formed in other reactions. Fusion reactions have also been used to try produce super-heavy nuclei and to produce proton rich nuclei very far from the stability line.

There are important features of fusion reactions. For light projectiles and low incident energies the fusion cross-section may be a considerable fraction of the reaction cross-section. The second important feature is, with increasing charge of the interacting ions the fusion probability falls abruptly. The other feature of fusion reaction is the fusion cross-section at first increases linearly with $\mathbf{1/E_{CM}}$, reaches a maximum and thereafter decrease linearly with $\mathbf{1/E_{CM}}$.The detailed energy dependence of the fusion cross-section may differ quite considerably for different interacting ions forming the compound nucleus. In general, the fusion cross-section varies quite smoothly with the energy, but in the case of light systems it may show quite large oscillations. When two heavy ions fuse, they form a compound nucleus which is far from statistical equilibrium since a large fraction of its energy is in form of an orderly collective translational motion of the nucleons of the projectile and the target. This orderly motion transforms into chaotic thermal motion through a cascade of nucleon-nucleon interactions during the thermalization of the compound nucleus. This takes some time and before reaching thermal equilibrium, nucleons or clusters of which still have energy considerably higher than their equilibrium thermal energy may be emitted into the continuum.

2.4.2 Incomplete Fusion of HI

Incomplete fusion reaction [1, 2, 3, 9, 10, 11] is a reaction where fractional mass, charge and momentum of the projectile are transferred to the target nucleus due to the prompt emission of projectile fragment(s) in the forward direction with almost projectile velocity.

The importance of this process is revealed by the study of excitation functions of reactions induced by complex projectile. Incomplete fusion reaction has also been observed in the interaction of light ions such as ^{12}**C,** ^{14}**N** and^{16}**O** with heavy targets. These ions may break-up preferentially into α-type fragments (for instance, in the case of Nitrogen it may break-up in to ^{10}**B** and α-particle or ^{6}**Li** and two **α**-particles) where one of which further fuses with the target nucleus. The contribution of the incomplete fusion cross-sections may be separated from the complete fusion in several ways.

The first evidence for such phenomena was found by measuring the angular correlation of fission fragments. Fusion reactions lead to emission of fragments at relative less angles and are the dominant contribution at all the energies considered, but, with a probability increasing with energy, almost back-to-back fragment emissions are also observed. This may only occur if, as in incomplete fusion, a momentum considerably smaller than that of the projectile is transferred to the fissioning compound nucleus. Further experiments measured the incomplete fusion cross-section by detecting the spectator fragment in coincidence with the γ-lines of the incomplete fusion residue or by measuring (by activation techniques) the recoil ranges and the angular distribution of the incomplete fusion residues.

These last experiments are based on the consideration that a compound nucleus formed in an incomplete fusion reaction has, respectively, a smaller linear momentum and a larger recoil angle than a compound nucleus formed in a complete fusion process.

2.5 Nuclear Reactions and Models

Many recent [12] heavy-ion experiments have provided evidence for non-equilibrium particle emission. An appropriate reaction model is necessary to interpret the physical message that the experimental observations convey. If the model has the important parameters properly included, the interpretation of the observations may lead to understanding. Suitable models for heavy-ion pre-compound decay phenomena may provide the necessary bridge in understanding the transition between low energy compound nucleus reactions and the fragmentation reactions of higher incident energies. Among the several semi-classical models which have been proposed in reproducing a large body of experimental data are the Hybrid and Geometry Dependent Hybrid models. They have been reasonably successful in reproducing a broad range of experimental data. This was accomplished with several choices of parameter options. Recently quantum mechanical theories of pre-equilibrium emission have been proposed. These quantum mechanical models provide, in principle, way of calculating the cross-sections of pre-equilibrium processes without the uncertainties of the semi-classical approximations. These models are in the early stage of application, at the present. Even for light heavy-ion particle α, the quantum mechanical treatment of the initial particle-target interaction become very complicated.

2.5.1 Intra-nuclear Cascade Model (INC)

The Intra-nuclear cascade model [12] was first proposed by Serber and first implemented to explain the interactions of high energy neutrons with complex nuclei. In INC model the projectile enters the target nucleus with a given parameter **b**. The projectile interacts with the target nucleons after travelling a certain distance inside the target nucleus, and excites it above the Fermi Gaz. Each scattered particle then travel through the nucleus interacting with the other nucleons.

The INC model traces the individual nucleon trajectories in three-dimensional geometry. The trajectories of all excited particle are followed until some arbitrary energy significantly above the mean equilibrium value has been attained by the nucleon. Particles reaching the nuclear surface with sufficient energy are assumed to be emitted. When all particles of a given cascade have been traced, the total energy of the residual nuclei, its identity, and the energies and angles of the emitted particles are shared, and a new cascade with new impact parameter is calculated with help of such an approach, the time evolution of the reaction can be generated but after few collisions the actual calculations becomes too much complicated. The INC model is a realistic model but in general, the model prediction is not satisfactorily at backward angles and is some forward angles also.

2.5.2 Harp-Miller-Berne Model

In Harp-Miller-Berne model [12], the nuclear single particle states are classified according to their energies in groups or **bins** whose size **ΔE** is chosen to be of some convenient dimension.

In the calculations, the fractional occupation of each bin is taken as function of time. This model calculates the occupation probability of an average state in $\mathbf{i^{th}}$ bin as a function of time using Fermi gas distribution. At the initiation of the reaction, at the time $\boldsymbol{\tau_0}$ all the levels below the Fermi energy are filled up (as the target is in ground state), and the projectile is in an excited state. This gives the fractional occupation probability at time τ=τo. Two-body interactions then lead to a redistribution of probabilities.

After calculating the relative probabilities of scattering into and out of each bin and the emission from bins above the particle binding energies, populations of all bins are changed accordingly. The calculation is repeated until a steady state configuration is reached. At each time during the equilibrium process the energy spectrum of emitted nucleons are calculated and a net spectrum obtained.

Later by Harp and Miller in HMB model, a minor modification is suggested. They considered the nucleus to be composed of independent proton and neutron Fermi gases. Therefore, the proton and neutron occupation numbers for the single particle states of these gases completely specifies the internal configuration of the nucleus at any time. Further, it is also assumed that the mechanism for the equilibrium of the gases takes place through binary nucleon-nucleon collisions. Correspondingly a new set of master equation is obtained, the solution of which gives the proton and neutron occupation numbers.

2.5.3 The Exciton Model

The Exciton Model [1, 12] is first introduced by Griffin in 1996 and later modified by many workers. In the Exciton model, the compound nucleus states are characterized by the number of excited particles and holes (the excitons) at any stage of the nucleon-nucleon cascade. In this model the equilibration between target and projectile is achieved by the succession of nucleon-nucleon interactions. An excited nucleus is considered as a gas of quasi-particles i.e., particle-hole degree of freedom is included.

The initial configuration is fixed by the nature of the projectile. For instance in case of a nucleon-induced reaction, it is a two-particle-one hole configuration due to the interaction of the incident nucleon with a nucleon of the target which is excited from a state below to a state above the Fermi energy. Additional two-body interactions

give rise to a sequence of states characterized by increasing exciton numbers, eventually leading to a fully equilibrated residual nucleus.

Restriction to two-body interactions leads to the following section rules concerning the possible variation of the number of particles, p, hole, h, and excitons, **n=p+h**, in the course of the cascade of interactions: **Δp=0, ±1 Δh=0, ±1 Δn=0, ±2**

The states which are excited in the course of this interaction cascade are very unstable. In exciton model intermediate states play significant role in dealing with PE processes.

Single particles densities are often used to calculate the exciton level densities, assuming the nucleus to be distinguishable Fermi gas with equidistance level. The transition rates are proportional to level density of the final accessible states (Fermi Golden rule). Ericson's level density result, at a given exciton number, n with excitation energy $\mathbf{E_{ex}}$ is

$$\boldsymbol{\varphi_n(E_{ex})} = \frac{\mathbf{g(gE_{ex})^{p+h-1}}}{\mathbf{p!h!(p+h-1)!}}$$

in this equation g is the one-particle state density**,** $\mathbf{E_{ex}}$ is the excitation energy, and p and h are the number of excited particles and holes respectively. William gave expression for the particle-hole density by considering the effect of the Pauli exclusive principle in the uniform spacing model as

$$\boldsymbol{\varphi_n(E_{ex}) = \varphi_n(E_{ex})} = \frac{\mathbf{g(gE_{ex}-A(p,h))^{p+h-1}}}{\mathbf{p!h!(p+h-1)!}}$$

Where $\mathbf{A\ (p,h) = (p^2 + h^2 + p - h) - \frac{1}{2}h}$.

The probability of decay from an n exciton state $\boldsymbol{\varphi_n(E_{ex})}$ is defined as the ratio of the emission rate from n to the rates of all transitions (including emission) from n. If $\boldsymbol{\lambda_c^n(\varepsilon)}$ be the emission rate with energy ε (in the interval dε) from the n exciton state and $\boldsymbol{\lambda^n}$ **±,0** the probabilities for the transitions corresponding to the charge of the exciton number **Δn=±2, 0**

$$\boldsymbol{\varphi_{n(\varepsilon)}} = \frac{\boldsymbol{\lambda_c^n(\varepsilon)}}{\boldsymbol{\lambda_+^n + \lambda_-^n + \lambda_0^n + \int d\varepsilon \lambda_c^n(\varepsilon)}}$$

The exciton model assume that (1) at each stage of the cascade all the states with the same configuration and the same total energy are equi-probable, and (2) at each stage of the cascade all the processes which may occur are also equi-probable.

The first assumption implies that partitioning of energy occurs with equal probability. Hence emission rates are summed over all ε in the denominator to obtain $\varphi_n(\varepsilon)$. The emission rates as obtained from the principle of detailed balance is given by

$$\lambda_c^n(\varepsilon) = \frac{2s+1}{\hbar}\left[\frac{\varphi_{n'}(u)}{\varphi_n(Eex)}\right] m\varepsilon\sigma_{inv}(\varepsilon)$$

here s and m are the intrinsic spin and reduced mass of the ejectile, n' is the exciton number after emission of ejectile with v nucleons: **n'=n-v**, u is the residual excitation energy given by **$u = E_{ex} - B - \varepsilon$**, with B the ejectile separation energy, **σ_{inv}** is the inverse cross-section. Using Fermi's Golden rule the transition rates are defined as

$$\lambda_+^n = \frac{2\pi}{\hbar}[M_+]^2\varphi_{n+2} \quad ,\Delta n=+2$$

$$\lambda_-^n = \frac{2\pi}{\hbar}[M_-]^2\varphi_{n-2} \quad ,\Delta n=-2$$

$$\lambda_0^n = \frac{2\pi}{\hbar}[M_0]^2\varphi_n, \Delta n=0$$

Here $[M_0,\pm]$are the matrix elements of the corresponding transitions.φ_{n+2},$\varphi_{n-2}$and$\varphi_n$are the density of states available in the **n+2**, **n-2**,and **n** exciton states after **Δn=2**,**-2** and **0** transitions. The estimation of the transition matrix element **[Mo, ±]** proves to be one of the most crucial points in the model. A common estimation is to assume **$M_+=M_-=M_0= M$**. Using the assumption and the consequent restriction imposed on, the density of final states, the transition states were given by Williams as

$$\lambda_+ = \frac{2\pi}{\hbar}[M]^2\frac{g^3E^2}{2(n+1)}, \Delta n=+2$$

$$\lambda_0 = \frac{2\pi}{\hbar}[M]^2 g^2 E\frac{3n-2}{4} \quad ,\Delta n=0$$

$$\lambda_- = \frac{2\pi}{\hbar}[M]^2 gph\ (n-2)\ ,\ \Delta n=-2$$where E is the excitation energy of the system. Compound nuclear equilibration is attained when the rate of creation of p-h pairs approximately equals the annihilation rates of such pair, so that the exciton number **n=n'** remains unchanged. Assuming that **$\lambda_{n+2} = \lambda_{n-2} = \lambda_0$** equilibrium i.e., **n=n'** it follows **$n' \cong \sqrt{2gE}$**

At low excitation energy, it is reasonable to assume energy independent matrix element, while at higher excitation energies, energy dependent matrix elements are used. The analysis of a large body of data indicates that a mass and energy dependence of the average square matrix foe nucleon-nucleon interaction given by Kalback's estimate, according to which $[M]^2$ has the following mass number A and energy Eex dependent **$[M]^2 = KA^{-3}E_{ex}^{-1}$** where k is an adjustable parameter ranging from 95-700 MeV.

2.5.4 The Hybrid Model

A decade ago predictions of pre-equilibrium decay in heavy ion reactions were made by using the hybrid model [12].

2.5.5 Geometry Dependent Hybrid Model

Geometry dependent hybrid (GDH) model [12] has been reasonably successful in reproducing a broad range of data. This was accomplished with several choices of parameter options. The geometry dependent hybrid model is a variant of the HM in which the nuclear geometry effects are considered. GDH model takes into account the reduced matter density and hence also the shallow potential. In this way the diffused surface properties sampled by higher impact parameter were incorporated into the pre-compound decay formalism in the geometry dependent hybrid model.

The nucleon density distribution in the nuclear skin can affect the pre-equilibrium decay in two ways. First the mean free path in the intra-nuclear transitions is greater in the diffused edges and secondly the Fermi energy will be lower in that region so that the hole depth is limited. Considering these effects the hybrid model for the cross sections was reformulated as a sum of contributions over impact parameter.

III. EXPERIMENTAL DETAILS

The experiment [5] was conducted at Inter-University Accelerator Centre, New Delhi, India, where data are found in EXFOR web site. It is not possible to conduct the experiment here in Ethiopia since there is no such facility available. So there is no experimental result available for comparison.

3.1 Experimental Method

The typical experimental arrangement for the study of nuclear reactions is an accelerator producing a collimated mono-energetic beam, a target containing the nuclei being studied and detectors of the emerging particles (ejectiles) of the delayed radiations.

The quantity one measures most frequently is the energy distribution of particles emitted at a given angle, the so called double differential spectra, which may be integrated over the angle to provide the angle integrated spectra.

The excitation function is also one of the quantities one measures most frequently. Excitation function is the angle integrated cross-section for a given reaction as a function of the projectile energy. Excitation function is very easily measured when the reaction produces a radioactive residue, by detecting the activity induced in the target and/or a set of absorbers downstream from the target. This gives the number of residues which are produced from which one deduce the total cross-section for the reaction concerned.

In this study, the fusion and transfer cross-sections were determined by the in-beam and off-beam gamma ray spectroscopy methods, which allow the simultaneous measurement of fusion, transfer channels and inelastic scattering cross-sections. The transfer cross-sections determined are a lower limit of the total transfer yield, since they corresponds to transfer processes leading to the excited states from which gamma transitions are detected.

Experimentally, the cross-section $\sigma_r(E)$ at a given energy E for different reactions was determined using the expression,

$$\boldsymbol{\sigma_r(E) = \frac{c\lambda e^{\lambda t_1}}{No\xi\varphi\theta Ge(1-e^{-\lambda t_i})(1-e^{-\lambda t})}}$$

Where cλ is activity of the isotope produced in the reaction, t_1 the time lapse between the end of irradiation and the start of the counting, λ the decay constant of

the isotope produced, $N_0$is the number of target nuclei irradiated in the time interval t_i,$\boldsymbol{\varphi}$is the incident flux, θ is the branchingratio of identified γ-ray, and $\mathbf{G_e}$ is the geometry dependent efficiency of the detector for a particular energy E.

The quantity **ξ** is the correction for self-absorption of the γ-ray with absorption coefficient μ for the sample of thickness d, and it is given as

$$\boldsymbol{\xi} = \frac{\mathbf{1-e^{-\mu d}}}{\boldsymbol{\mu d}}$$

3.2 Sample preparation

In the sample, the target consisted of pure metallic Cobalt, with thickness in the range 200-400 mu-g/cm^{-2}, evaporated on Pb backings thick enough to stop the beam, in order to avoid Doppler shifts of the gamma-lines. For each bombarding energy, a different target was used, avoiding undesirable contributions to the spectra coming from the decay of previous irradiations.

3.3 Experimental Errors

There were experimental errors in the value of the fusion cross-sections due to (1) statistical errors in the determination of the gamma yields, (2) systematic errors due to the target thickness, absolute efficiency and faraday-cup or thick target calculation for coulomb excitation and (3) errors from the contaminants corrections. The overall error is in the range from 8% at higher energies to almost 20% at very low energies.

IV.THE COMPUTER CODES AND FORMULATION

4.1 Analysis with Computer Codes

In a compound nucleus reaction [1] two nuclei fuse together to form an excited composite nucleus, which then decays either through particle and/or γ-ray emission or by the process of fission. Formation of the compound nucleus is inhibited primarily by the electrostatic repulsion between the collision partners. At energies above the Coulomb barrier, the analysis of a complex interaction such as the compound nucleus formation and its subsequent decay could be explained through the application of statistical theory. Various computer codes viz., PACE4, CASCADE, ALICE91 and SUMRULE are available to perform such statistical model calculations. In the following sections, a brief description of two those codes are presented.

4.1 .1 PACE4

The statistical model code Projection-Angular-Momentum-Coupled- Evaporation (PACE4) [2] is derived from the original code called JULIAN. It uses a Monte-Carlo procedure to determine the decay sequence of an excited nucleus using the Hauser-Feshbach formalism. The main advantage of Monte-Carlo calculations is to provide correlations between various quantities, such as particles and gamma-rays, or angular distribution of particles. Sequential decays are considered until any further decay is prohibited due to the energy and angular momentum conservation laws.

A random number selection determines the actual final state to which the nucleus decays to and the process is, then repeated for other cascades until all the nuclei reach the ground state. The transmission coefficients for light particle emission (n, p, α) are determined using optical model potentials. A fission decay mode is employed using a rotating liquid drop fission barrier routine.

The code also provides event by event trace back of the entire decay sequence from the compound nucleus into any one of the exit channels. The fusion cross-sections are obtained from the Bass model. There are two default level density options that are essentially derived from the Fermi gas formalism and are identical to constant temperature formalism at low energies. These are i) the determination of the parameter ‘a’ and ii) ‘a’ is taken to be equal to A/K, where, A is the number of nucleons and K is constant factor(a free parameter),its value may be varied to match the experimental data. Independent of these options, rotational energy contribution

E_{rot}(J) can be selected in two ways viz., the spin cut-off parameter and the ground-state rotational energy of the finite-range rotating-drop model. For values of A, Z or J beyond the range of validity of Sierk's routine, the rotational energies are taken from the work of Cohen, Plasil and Swiatecki.

The partial cross-section for CN formation at angular momentum (l) and specific bombarding energy is given by,

$$\boldsymbol{\sigma_l = \frac{\pi\lambda^2}{4\pi^2}(2l+1)T_l}$$

where, λ is the reduced wavelength and T_l , the transmission coefficient given by

$$\boldsymbol{T_l = [1+\exp(l - l_{max})/\delta]^{-1}}$$

where, δ is the diffuseness parameter and $l_{max}$is determined by the total fusion cross-section σ_F , since,

$$\boldsymbol{\sigma_F = \sum_{l=0}^{\infty} \sigma_l}$$

It may be pointed out that code PACE4 performs only the statistical equilibrium model calculations and does not take pre-equilibrium (PE) and in-complete fusion processes into consideration.

4.1.1.1 Analysis with Computer code PACE4

The PACE4 [2] code is based on a statistical approach. In this program the de-excitation of the compound nucleus is followed by a Monte-Carlo procedure. The angular momentum projections are calculated at each stage of de-excitation, which enables the de-excitation of the angular distribution of the emitted particles. The level density parameter is an important parameter which may be varied to match the experimental data. The effect of variation in the level density parameter constant 'k' on calculated excitation functions for the $^{59}_{27}\mathrm{Co}(^{20}_{10}\mathrm{Ne},\mathrm{pn})^{77}_{36}\mathrm{Kr}$ reaction is shown in below as can be observed from this figure, a value of 'k'=16 satisfactorily reproduce the measured excitation functions.

ENERGIES	CROSS-SECTION(MB)	Err(mb)	K=16	K=14	K=12
62.9	113.1	10.7	123.5	101.23	100.02
75.2	22	2.1	24.033	18.85	17.56
86.5	0.5	0.1	0.589	0.298	0.195

TAB4- 1: Theoretical and Measured cross-section for the reaction $^{59}_{27}\mathrm{Co}(^{20}_{10}\mathrm{Ne},\mathrm{pn})^{77}_{36}\mathrm{Kr}$used for studying the effect of the value of "k" on theoretically calculated results

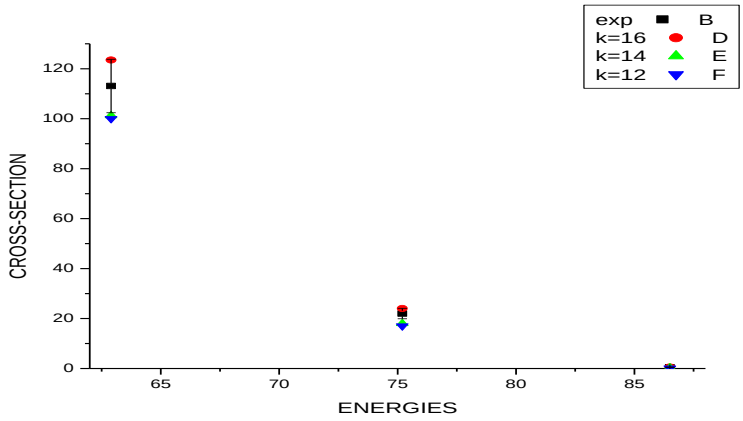

FIG4- 1: Excitation function for the reaction $^{59}_{27}\mathrm{Co}(^{20}_{10}\mathrm{Ne}, \mathrm{pn})^{77}_{36}\mathrm{Kr}$used for studying the effect of the value of "k" on theoretically calculated results

4.1.2 COMPLET

The code COMPLET [6] is a nuclear reactions code which was designed for versatility and ease of use in the bombarding energy range of few Mev to several hundred MeV. The code COMPLET is based on same philosophy as the former code INDEX. It applies the statistical model of compound nucleus decay developed by Weisskopf-Ewing and the hybrid and geometric dependent hybrid model of Blann and the further simplification and improvement by Ernst [12].

It predicts the yield of residual nuclei in nuclear reaction with excitation energy up to 225MeV taking in to account two mechanisms. Pre-equilibrium emission is accompanied in the frames of the model of independently interacting exciton.

4.1.2.1 Analysis with Computer code COMPLET

The COMPLET code, originally, has been developed out of the code overlaid Alice by M.Blann. In this code, while some standard routines remained particularly unchanged (like FISROT, LYMASS, PUNCH, PLT, PARAP, OVER1, OVER2 and TLJ) others have been substantially modified (like MAIN, SHAFT, NUCMFP, etc) or are completely new (like INDEX, PARDEN, TRAPRO, ANGULAR, etc).The COMPLET code includes damping of fission widths above a critical temperature, rotating liquid drop fission barriers and rotational energies due to Seirk included for jcal=0. Still M&S or Exp. Masses are used as before. The code COMPLET includes pre-equilibrium neutron, proton and alpha emission up to two particles as well as evaporation of neutron, proton, alpha, deuterons, tritons and hellions. The COMPLET code is based on the Weisskopf-Ewing model [1,2] for compound nucleus calculations and the Hybrid model for simulating pre-equilibrium emission. The code assumes equi-partition of energy among the initially excited particles and holes. The code uses Gove mass

tables or the Myers Swiatecki/Lysekil mass formula. The option that substitutes Gove's table for Myers Swiatecki/Lysekil mass formula including shell corrections was used. In order to calculate inverse cross-sections, the optical model subroutine with the parameters of Becchetti and Greenless was employed.

The important parameters of the COMPLET code are the level density parameter a, initial exciton number n_0, and the mean free path multiplier CMFP. The first parameter greatly affects the equilibrium component, through the level densities. The level density parameter 'a' is calculated using the relation a=A/k, where A is the mass number of the compound system and k is a constant which may be varied to match the experimental data. The parameter n_0 and CMFP greatly govern the pre-equilibrium component.

The initial exciton number n_0 decides the complexity of the initial configuration. A smaller value of n_0, means that the initial state is less complex and hence far from the equilibrium. As such, a larger pre-equilibrium contribution is expected. On the other hand, a large value of n_0, means that the system is nearer to the equilibrium stage and therefore, small pre-equilibrium contribution is likely.

In order to see the effect of variation of n_0 calculated excitation functions, calculations were done by varying n_0 from 20 to 22. As a representative case, these calculations for ${}^{59}_{27}\mathrm{Co}({}^{20}_{10}\mathrm{Ne},\alpha){}^{75}_{35}\mathrm{Br}$ channel are shown in Figure below. It may be seen from this figure that a value of n_0 =20 is best suited for the present experimental data, even though the effect is not as such significant as shown, clearly, in the figure. The value of n_0 =20 may be justified assuming that the projectile 20N breaks up in the nuclear field of the target nucleus creating 20 excitons.

ENERGIES	CROSS-SECTION(mb)	Err(mb)	n_0=20	n_0=21	n_0=22
75.2	91.3	8.4	91.9	106	107.9
80	--	--	135	145	--
85	--	--	162	172	--
86.5	174.9	11.8	169	199.89	200.96
90	--	--	157	166.23	--
95	--	--	154	160.35	--
97.1	164.2	15.7	155.98	200.85	206.23
100	--	--	135	142.3	--
107	84.3	5.7	80.55	102	100.55

TAB4- 2: Theoretical and Measured cross-section for the reaction ${}^{59}_{27}\mathrm{Co}({}^{20}_{10}\mathrm{Ne},\alpha){}^{75}_{35}\mathrm{Br}$ used for studying the effect of exciton number n_0 on theoretically calculated results

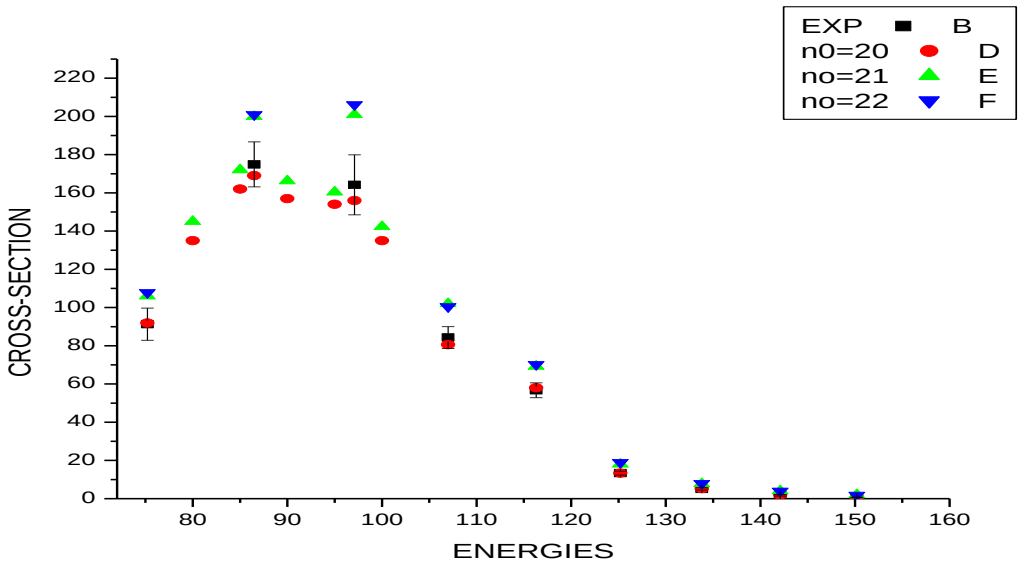

FIG4- 2: Excitation function for the reaction $^{59}_{27}\mathrm{Co}(^{20}_{10}\mathrm{Ne},\alpha)^{75}_{35}\mathrm{Br}$ used for studying the effect of exciton number n_o on theoretically calculated results

The parameter CMFP, which is used to adjust the mean free path for two-body residual interactions inside the nuclear matter, is varied from 1 to 4 and its effects on excitation function for $^{59}_{27}\mathrm{Co}(^{20}_{10}\mathrm{Ne},\alpha)^{75}_{35}\mathrm{Br}$ reaction is shown in figure below, as a representative case. The value of CMFP=1 is best suited for the present experimental data.

ENERGIES	CROSS-SECTION(mb)	Err(mb)	CMFP=1	CMFP=2	CMFP=3	CMFP=4
75.2	91.3	8.4	91.9	102.9	104.23	107.8
80	--	--	135	145	--	
85	--	--	162	172	--	
86.5	174.9	11.8	169	190.14	193.06	195.23
90	--	--	157	166.23	--	
95	--	--	154	160.35	--	
97.1	164.2	15.7	155.98	182.56	185.75	188.12
100	--	--	135	142.3	--	
107	84.3	5.7	80.55	95.6	97	99.99

TAB4- 3: Theoretical and Measured cross-section for the reaction $^{59}_{27}\mathrm{Co}(^{20}_{10}\mathrm{Ne},\alpha)^{75}_{35}\mathrm{Br}$ used for studying the effect of CMFP parameter on theoretically calculated results

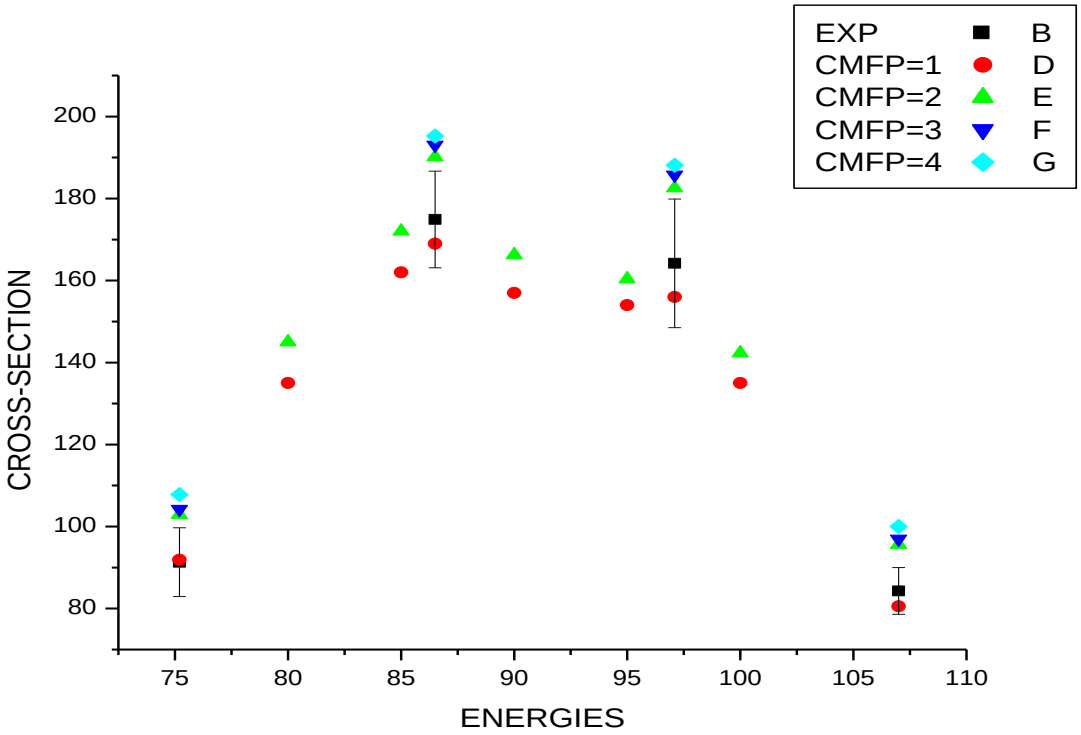

FIG4- 3: Excitation function for the reaction $^{59}_{27}\mathrm{Co}(^{20}_{10}\mathrm{Ne},\alpha)^{75}_{35}\mathrm{Br}$ used for studying the effect of CMFP parameter on theoretically calculated results

The effect of the variation of 'k' on the calculated excitation functions was also studied. The value of 'k' was varied from 12 to 16. As a typical example, the calculated excitation functions for the $^{59}_{27}\mathrm{Co}(^{20}_{10}\mathrm{Ne},\alpha)^{75}_{35}\mathrm{Br}$ reaction for different values of 'k' are shown in the fig below. As can be seen from this figure, and in general also, the present experimental data is best reproduced with a value of 'k'=16

ENERGIES	CROSS-SECTION(mb)	Err(mb)	K=16	K=14	K=12
75.2	91.3	8.4	91.9	80.12	79
80	--	--	135		
85	--	--	162		
86.5	174.9	11.8	169	160.22	158.02
90	--	--	157		
95	--	--	154		
97.1	164.2	15.7	155.98	146.25	144
100	--	--	135		
107	84.3	5.7	80.55	74	72.45

TAB4- 4: Theoretical and Measured cross-section for the reaction $^{59}_{27}\mathrm{Co}(^{20}_{10}\mathrm{Ne},\alpha)^{75}_{35}\mathrm{Br}$ used for studying the effect of the value of "k" on theoretically calculated results

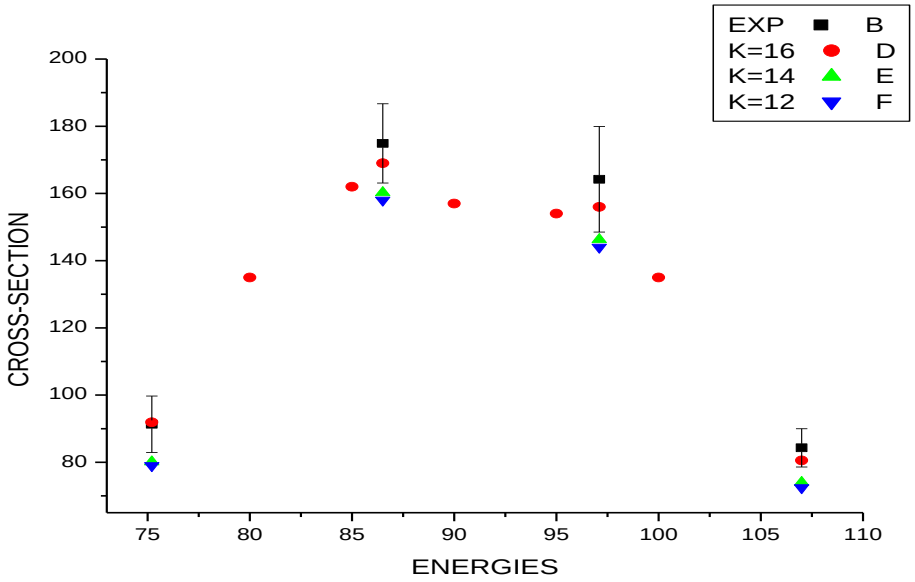

FIG4- 4:Excitation function for the reaction $^{59}_{27}\mathrm{Co}(^{20}_{10}\mathrm{Ne},\alpha)^{75}_{35}\mathrm{Br}$ used for studying the effect of the value of "k" on theoretically calculated results

V. RESULT AND DISCUSSION

In the present work the excitation functions for several residues were studied, these are: ${}^{59}_{27}\mathrm{Co}({}^{20}_{10}\mathrm{Ne}, \mathrm{pn})^{77}_{36}\mathrm{Kr}$, ${}^{59}_{27}\mathrm{Co}({}^{20}_{10}\mathrm{Ne}, \mathrm{p2n})^{76}_{36}\mathrm{Kr}$, ${}^{59}_{27}\mathrm{Co}({}^{20}_{10}\mathrm{Ne}, 2\mathrm{pn})^{76}_{35}\mathrm{Br}$, ${}^{59}_{27}\mathrm{Co}({}^{20}_{10}\mathrm{Ne}, \alpha)^{75}_{35}\mathrm{Br}$, ${}^{59}_{27}\mathrm{Co}({}^{20}_{10}\mathrm{Ne}, \alpha 2\mathrm{n})^{74}_{35}\mathrm{Br}$, ${}^{59}_{27}\mathrm{Co}({}^{20}_{10}\mathrm{Ne}, \mathrm{p}\alpha\mathrm{n})^{73}_{34}\mathrm{Se}$, ${}^{59}_{27}\mathrm{Co}({}^{20}_{10}\mathrm{Ne}, \alpha \mathrm{p}4\mathrm{n})^{70}_{34}\mathrm{Se}$, ${}^{59}_{27}\mathrm{Co}({}^{20}_{10}\mathrm{Ne}, 2\mathrm{p}\alpha\mathrm{n})^{72}_{33}\mathrm{As}$, ${}^{59}_{27}\mathrm{Co}({}^{20}_{10}\mathrm{Ne}, 2\alpha)^{71}_{33}\mathrm{As}$, ${}^{59}_{27}\mathrm{Co}({}^{20}_{10}\mathrm{Ne}, 2\alpha\mathrm{n})^{70}_{33}\mathrm{As}$, ${}^{59}_{27}\mathrm{Co}({}^{20}_{10}\mathrm{Ne}, 2\alpha\mathrm{pn})^{69}_{32}\mathrm{Ge}$, ${}^{59}_{27}\mathrm{Co}({}^{20}_{10}\mathrm{Ne}, 2\alpha 2\mathrm{p}2\mathrm{n})^{67}_{31}\mathrm{Ga}$, ${}^{59}_{27}\mathrm{Co}({}^{20}_{10}\mathrm{Ne}, 3\alpha\mathrm{p})^{66}_{31}\mathrm{Ga}$, ${}^{59}_{27}\mathrm{Co}({}^{20}_{10}\mathrm{Ne}, 3\alpha 2\mathrm{p}2\mathrm{n})^{61}_{29}\mathrm{Cu}$, These were carried out in the incident energy range 62.9-150.2 MeV.

The experimental excitation functions were compared with the theoretical predictions obtained from code PACE4, and COMPLET code. The experimental cross-section and energy are obtained from IAEA data source, EXFOR library [5].

The projectile energy is measured in Mega electrovolt (Mev) and the cross-section in millibarn (mb).

Energy range selected from the data is same with theoretical. The cross-section of theoretical and experimental with the energy range is given in the tables below.

V.1. Production of Residues

V.1.1.The production of Krypton

$$^{59}_{27}\mathrm{Co}(^{20}_{10}\mathrm{Ne},\mathrm{pn})^{77}_{36}\mathrm{Kr}$$

ENERGIES	CROSS-	Err(mb)	COMP	PRECOMP	PACE4
62.9	113.1	10.7	1.03E+02	9.92E+01	123.5
75.2	22	2.1	1.80E+01	1.53E+01	24.033
86.5	0.5	0.1	4.79E-01	3.46E-01	0.589

TAB5- 1: Theoretical and Measured cross-section for the reaction $^{59}_{27}\mathrm{Co}(^{20}_{10}\mathrm{Ne},\mathrm{pn})^{77}_{36}\mathrm{Kr}$

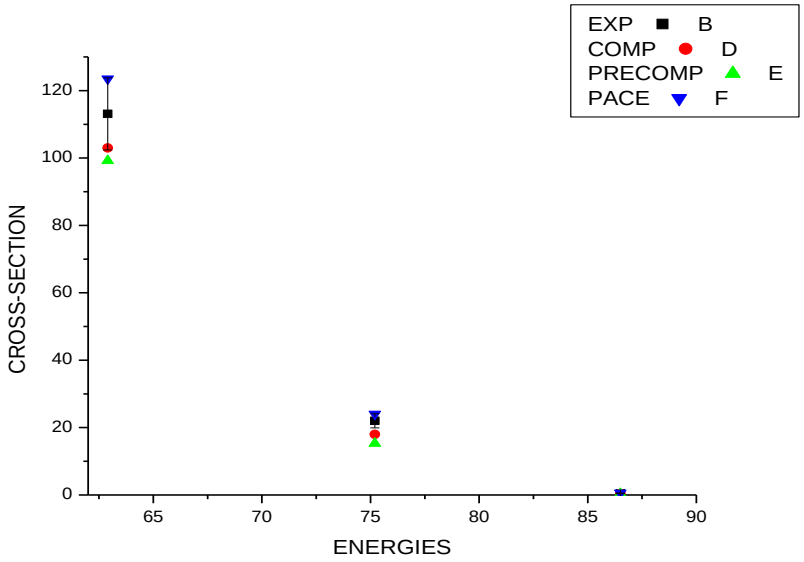

FIG5- 1: The production of Krypton $^{59}_{27}\mathrm{Co}(^{20}_{10}\mathrm{Ne},\mathrm{pn})^{77}_{36}\mathrm{Kr}$

In the reaction $^{59}_{27}\mathrm{Co}(^{20}_{10}\mathrm{Ne},\mathrm{pn})^{77}_{36}\mathrm{Kr}$ there is production of krypton $^{77}_{36}\mathrm{Kr}$ by emitting one proton and one neutron in the incident energies 62.9 -86.5 Mev. As shown in the graph above the theoretical cross sections calculated by PACE4 and COMPLET fit with the experimental cross sections at all projectile energies, especially PACE4 data. So in this reaction the projectile is assumed to fuse completely with the target nucleus forming the excited state ^{79}Rb*, and this excited state emits neutron and proton, during the thermalization, leaving behind the residual nucleus $^{77}_{36}Kr$. For this reaction the complete fusion reaction and pre-equilibrium emission contributions are more pronounced, and the discrepancy in experimentally measured cross-sections and theoretically calculated ones is less.

$$^{59}_{27}\mathrm{Co}(^{20}_{10}\mathrm{Ne}, \mathrm{p2n})^{76}_{36}\mathrm{Kr}$$

ENERGIES	σCROSS-SECTION(mb)	σErr(mb)	σCOMP	σPRECOMP	σPACE
62.9	72.7	3	4.60E+01	4.82E+01	5.52E+01
65			5.97E+01	6.20E+01	
70			6.92E+01	7.04E+01	
75			6.97E+01	7.03E+01	
75.2	147.6	4.9	7.58E+01	7.56E+01	8.61E+01
80			5.93E+01	6.68E+01	
85			4.83E+01	5.96E+01	
86.5	45.2	1.8	4.58E+01	3.89E+01	4.70E+01
90			2.88E+01	3.50E+01	
95			1.81E+01	2.24E+01	
97.1	15.5	0.7	1.52E+01	1.07E+01	1.61E+01
100			1.20E+01	8.07E+00	
107	1.9	0.3	2.12E+00	1.00E+00	2.19E+01

TAB5- 2: Theoretical and Measured cross-section for the reaction $^{59}_{27}\mathrm{Co}(^{20}_{10}\mathrm{Ne}, \mathrm{p2n})^{76}_{36}\mathrm{Kr}$

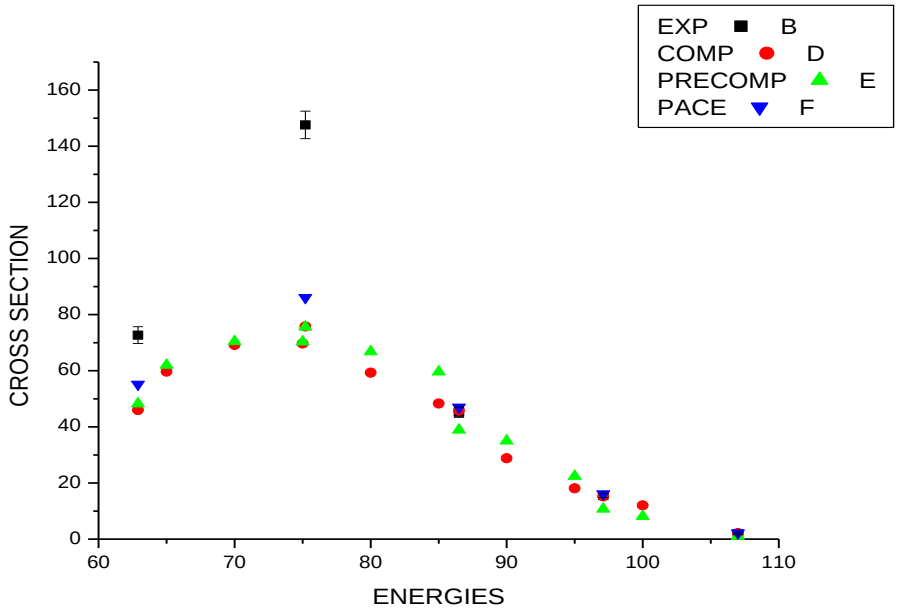

FIG5- 2: The production of Krypton $^{59}_{27}\mathrm{Co}(^{20}_{10}\mathrm{Ne}, \mathrm{p2n})^{76}_{36}\mathrm{Kr}$

In the reaction $^{59}_{27}\mathrm{Co}(^{20}_{10}\mathrm{Ne}, \mathrm{p2n})^{76}_{36}\mathrm{Kr}$ there is production of krypton $^{76}_{36}\mathrm{Kr}$ by emitting one proton and two neutrons in the incident energies 62.9 -107 Mev. Below 86.5 Mev the cross-sections don't fit, but above 86.5 Mev, the cross sections are fitting with experimental cross-sections. Theoretical calculations are almost comparable at higher energies with experimental data. From this observation, it is possible to explain this reaction as the complete fusion of the projectile with target. The reaction forms the excited state ^{79}Rb*, where this excited state emits two neutrons and one proton leaving behind the residual nucleus $^{76}_{36}\mathrm{Kr}$. In this reaction the contribution coming from complete fusion is more dominant. It can be seen from this figure that

the experimentally measured excitation function is close to the calculated theoretical excitation for the compound nucleus formation values calculated using COMPLET code or PACE4 code, both agree with experimental values. As such it may be possible to say that there is no pre-equilibrium emission at these energies. At 75 Mev the experimental value is very high and it's not explainable by any theoretical calculation. So maybe there is experimental error.

V.1.2.The production of Bromine

$$^{59}_{27}\mathrm{Co}(^{20}_{10}\mathrm{Ne}, 2\mathrm{pn})^{76}_{35}\mathrm{Br}$$

ENERGIES	σCROSS-SECTION(mb)	σErr(mb)	σCOMP	σPRECOMP	σPACE
62.9	107.2	7.2	1.11E+02	9.32E+01	1.14E+02
65			1.14E+02	1.16E+02	
70			1.37E+02	1.40E+02	
75			1.55E+02	1.57E+02	
75.2	182.7	12.3	1.77E+02	1.48E+02	1.95E+02
80			1.39E+02	1.38E+02	
85			1.01E+02	9.90E+01	
86.5	96.8	6.5	9.38E+01	8.27E+01	1.03E+02
90			7.22E+01	6.98E+01	
95			5.93E+01	5.64E+01	
97.1	14.2	1	1.39E+01	6.96E+00	1.51E+01
100			1.05E+01	4.67E+00	
107	2.3	0.2	2.20E+00	1.25E-01	
116.3	0.4	0.1	4.23E-01	2.23E-01	5.55E-01

TAB5- 3: Theoretical and Measured cross-section for the reaction $^{59}_{27}\mathrm{Co}(^{20}_{10}\mathrm{Ne}, 2\mathrm{pn})^{76}_{35}\mathrm{Br}$

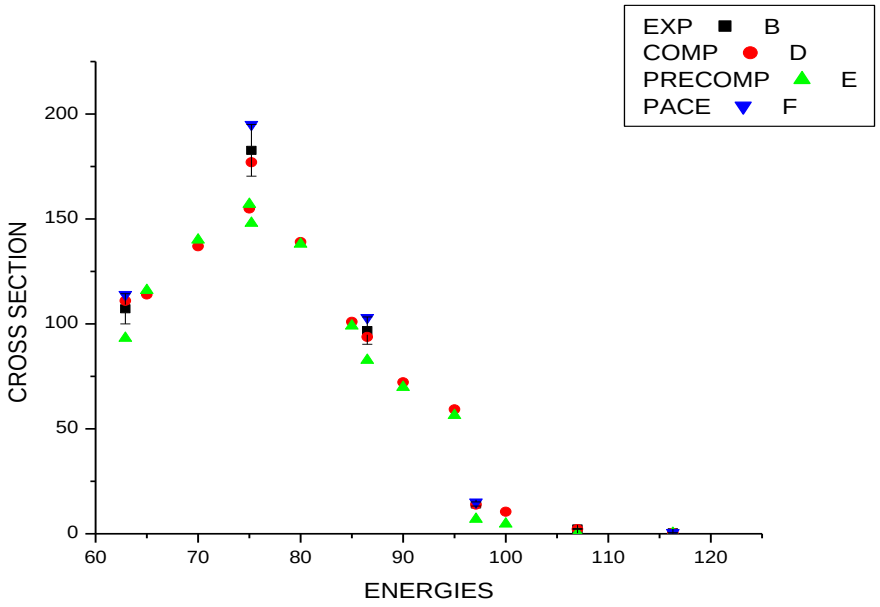

FIG5- 3: The production of Bromine $^{59}_{27}\mathrm{Co}(^{20}_{10}\mathrm{Ne}, 2\mathrm{pn})^{76}_{35}\mathrm{Br}$

In the reaction $^{59}_{27}\mathrm{Co}(^{20}_{10}\mathrm{Ne}, 2\mathrm{pn})^{76}_{35}\mathrm{Br}$ there is production of Bromine $^{76}_{35}\mathrm{Br}$ by emitting two protons and one neutron in the incident energies 62.9 -107MeV. As shown graph above the theoretical cross sections calculated by PACE4 and COMPLET-CN fit with the experimental cross sections at all projectile energies. However, the PACE4 values

are higher than the values calculated using COMPLET-CN. So in this reaction the projectile is assumed to fuse completely with the target nucleus forming the excited state ^{79}Rb*, and this excited state emits neutron and two proton, during the thermalization, leaving behind the residual nucleus $^{76}_{35}\mathrm{Br}$. Calculation base on COMPLET code including pre-equilibrium contribution are smaller than the experimental values almost at all the energies. The compound nucleus formation is seen even at energies around 100Mev for $^{20}_{10}\mathrm{Ne}$ and $^{59}_{27}\mathrm{Co}$ system.

$^{59}_{27}Co(^{20}_{10}Ne, \alpha)^{75}_{35}Br$

ENERGIES	CROSS – SECTION(mb)	Err(mb)	PRECOMP(mb)	COMP(mb)	PACE(mb)
75.2	91.3	8.4	91.9	78	77
80	--	--	135	142	--
85	--	--	162	170	--
86.5	174.9	11.8	169	150	149
90	--	--	157	165	--
95	--	--	154	160	--
97.1	164.2	15.7	155.98	130.24	128.33
100	--	--	135	138	--
107	84.3	5.7	80.55	104	102.6
116.3	56.7	3.9	58	30.6	35
125.2	13.4	1	13.4	10	9.14
133.8	5.1	0.6	5.25	3.01	3.05
142.1	1.8	0.4	2.02	1.2	1.09
150.2	0.7	0.1	0.797	0.696	0.59

TAB5- 4: Theoretical and Measured cross-section for the reaction $^{59}_{27}Co(^{20}_{10}Ne, \alpha)^{75}_{35}Br$

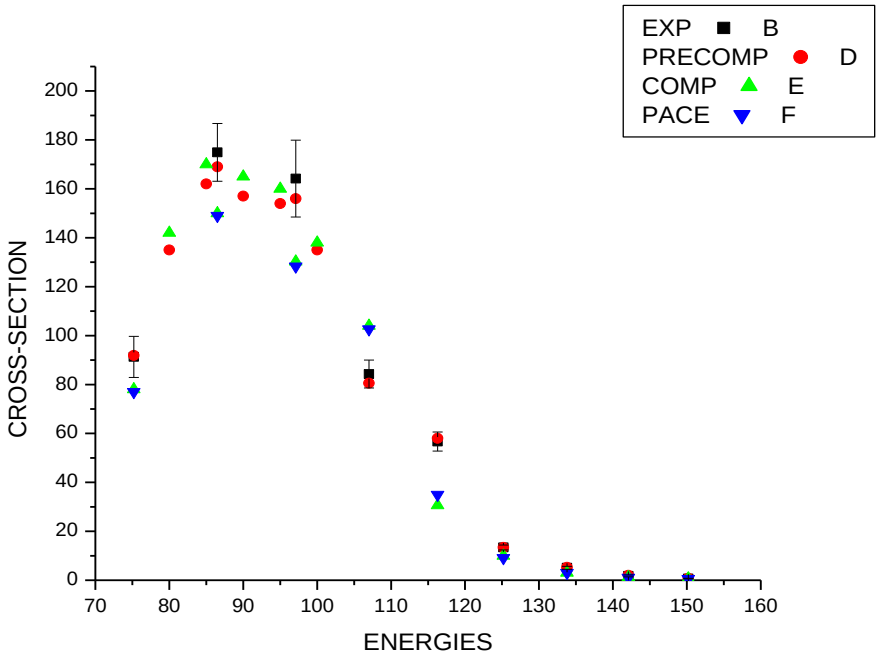

FIG5- 4: production of Bromine $^{59}_{27}Co(^{20}_{10}Ne, \alpha)^{75}_{35}Br$

In the reaction $^{59}_{27}Co(^{20}_{10}Ne, \alpha)^{75}_{35}Br$ there is production of Bromine $^{75}_{35}Br$ by emitting alpha in the incident energies 75.2 -150.2Mev. As shown in the graph above both PACE4 and COMPLET code give the values (Compound Nucleus formation) which are smaller than experimental values .Pre-equilibrium are better fit at all energies. This shows the signatures of pre-equilibrium decay in the (Ne, α) reaction. Alpha emitting channel is not explained by compound nucleus theory but pre-equilibrium decay.

$^{59}_{27}\mathrm{Co}(^{20}_{10}\mathrm{Ne}, \alpha 2\mathrm{n})^{74}_{35}\mathrm{Br}$

ENERGIES	σCROSS-SECTION	σErr(mb)	σPRECOMP	σCOMP	σPACE
75.2	62.2	8.4	56.6	50.1	49.21
86.5	108.2	13.1	108	88.1	87.55
97.1	171.8	17.8	170	143	142
107	210.6	20.6	211	135	133.44
116.3	253.4	24.8	232	300.56	302
125.2	141.2	15	151	178.23	180.01
133.8	123.4	12.9	131	157.03	158
142.1	86.1	14.3	87.8	99.2	102.55
150.2	60.5	9.1	62.1	88.2	90
75.2	62.2	8.4	56.6	50.1	49.21

TAB5- 5: Theoretical and Measured cross-section for the reaction $^{59}_{27}\mathrm{Co}(^{20}_{10}\mathrm{Ne}, \alpha 2\mathrm{n})^{74}_{35}\mathrm{Br}$

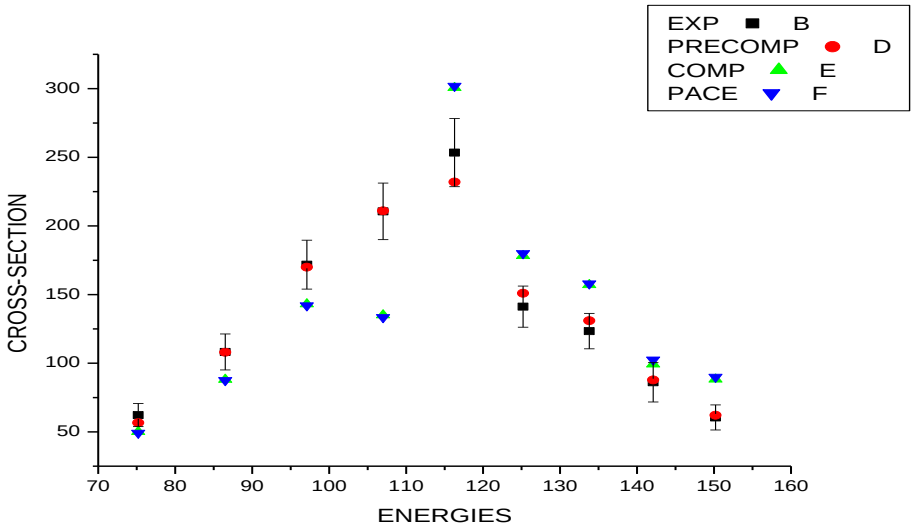

FIG5- 5: The production of Bromine $^{59}_{27}\mathrm{Co}(^{20}_{10}\mathrm{Ne}, \alpha 2\mathrm{n})^{74}_{35}\mathrm{Br}$

In the reaction $^{59}_{27}\mathrm{Co}(^{20}_{10}\mathrm{Ne}, \alpha 2\mathrm{n})^{74}_{35}\mathrm{Br}$ there is production of Bromine $^{74}_{35}\mathrm{Br}$ by emitting alpha and two neutrons in the incident energies 62.9 -150.2MeV. As shown in the graph above the theoretical cross sections calculated by PACE4 and COMPLET-CN don't fit with the experimental cross sections at all projectile energies. Again in this reaction, pre-equilibrium are better fit at lower and high energies.

V.1.3.The production of selenium

$$^{59}_{27}\mathrm{Co}(^{20}_{10}\mathrm{Ne},\alpha\mathrm{pn})^{73}_{34}\mathrm{Se}$$

ENERGIES	σCROSS-SECTION(mb)	σErr(mb)	σPRECOMP	σCOMP	σPACE
62.9	22.9	1.3	22.1	36	36.02
75.2	133.4	7.3	128	146	147
86.5	141	7.7	144	156	155
97.1	96.4	5.3	91.2	104	108
107	68.2	4.6	67.5	74.9	77.8
116.3	95.5	5.2	99.7	115	113
125.2	77.2	4.3	77.6	97.3	96.3
133.8	92.8	5.1	91.4	99	98
142.1	79	4.3	83	89.7	90.5
150.2	60.7	4.2	61.8	68.3	78

TAB5- 6: Theoretical and Measured cross-section for the reaction $^{59}_{27}\mathrm{Co}(^{20}_{10}\mathrm{Ne},\alpha\mathrm{pn})^{73}_{34}\mathrm{Se}$

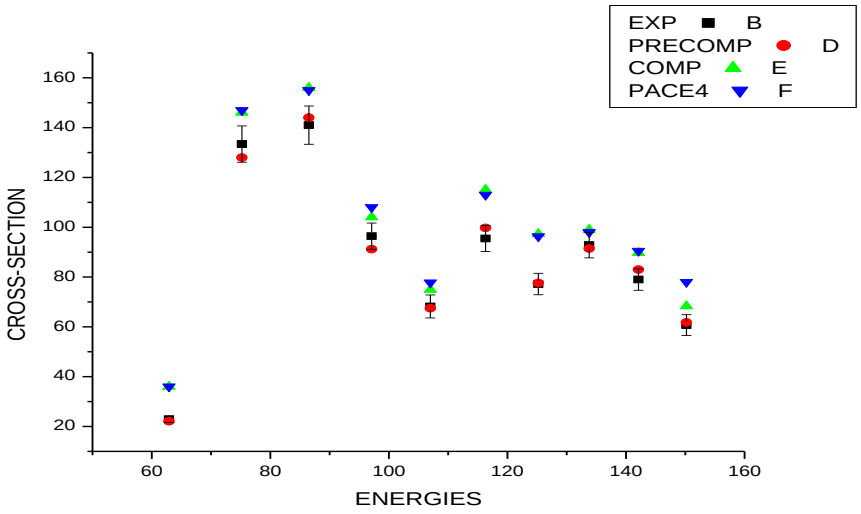

FIG5- 6: The production of Selenium $^{59}_{27}\mathrm{Co}(^{20}_{10}\mathrm{Ne},\alpha\mathrm{pn})^{73}_{34}\mathrm{Se}$

In the reaction $^{59}_{27}\mathrm{Co}(^{20}_{10}\mathrm{Ne},\mathrm{p}\alpha\mathrm{n})^{7\alpha3}_{34}\mathrm{Se}$ there is production of selenium $^{73}_{34}\mathrm{Se}$ by emitting alpha and proton and neutron in the incident energies 62.9 -150.2 Mev. As shown in the graph above the theoretical cross sections calculated by PACE4 and COMPLET-CN don't fit with the experimental cross sections at all projectile energies. The pre-compound nucleus values are in better agreement with experimental, while both compound values are higher.

$$^{59}_{27}\mathrm{Co}(^{20}_{10}\mathrm{Ne},\alpha\mathrm{p4n})^{70}_{34}\mathrm{Se}$$

ENERGIES	CROSS-SECTION	Err(mb)	COMP(mb)	PRECOMP(mb)	PACE(mb)
62.9	1.5	0.2	0	0	0
75.2	10.5	1.1	0	0	3.52E-06
86.5	12.3	1.5	3.54E-06	3.52E-06	1.23E-01
97.1	15.7	1.7	1.26E-01	1.23E-01	1.26E-01
107	21.2	7.8	2.77E+00	2.63E+00	9.58E+00
116.3	37	4.6	9.58E+00	8.92E+00	2.77E+00
125.2	42.3	6.2	1.31E+01	1.19E+01	3.54E-06

TAB5- 7: Theoretical and Measured cross-section for the reaction $^{59}_{27}\mathrm{Co}(^{20}_{10}\mathrm{Ne},\alpha\mathrm{p4n})^{70}_{34}\mathrm{Se}$

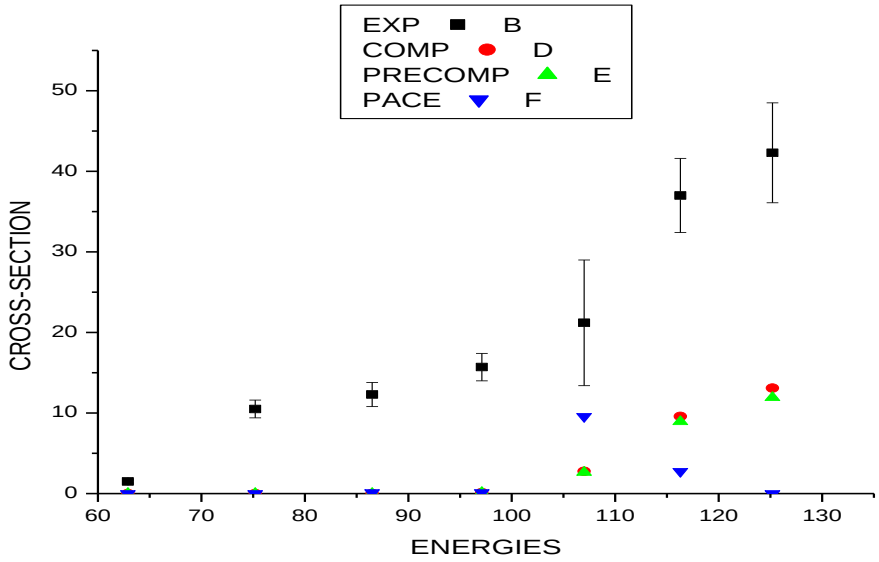

FIG5- 7: The production of Selenium $^{59}_{27}\mathrm{Co}(^{20}_{10}\mathrm{Ne},\alpha\mathrm{p4n})^{70}_{34}\mathrm{Se}$

As clearly shown in figure above for the $^{59}_{27}\mathrm{Co}(^{20}_{10}\mathrm{Ne},\alpha\mathrm{p4n})^{70}_{34}\mathrm{Se}$, experimental results are much higher than the theoretically calculated results using both codes. In this reaction the disagreement between the experimental and theoretical result can be resolved by assuming the projectile broken into alpha + ^{16}O.Alpha is emitted as spectator and ^{16}O is fused. The fusion of ^{16}O gives the compound nucleus formation which decays by the emission of p and 4n.Experimental values are much larger (about four times) than the compound or pre-compound nucleus calculation. At the higher energies where large number of particles emitted (six) and alpha is also emitted, it is seen that this is not explained by compound (PACE and COMPLET) or pre-compound calculations. This may be the case of incomplete fusion or direct reaction.

V.1.4.The production of Arsenic

$$^{59}_{27}\mathrm{Co}(^{20}_{10}\mathrm{Ne},\alpha 2\mathrm{pn})^{72}_{33}\mathrm{As}$$

In the reaction $^{59}_{27}\mathrm{Co}(^{20}_{10}\mathrm{Ne},2\mathrm{p}\alpha\mathrm{n})^{72}_{33}\mathrm{As}$ there is production of Arsenic $^{72}_{33}\mathrm{As}$ by emitting two proton, one neutron and alpha in the incident energies 75.2 -150.2MeV.

ENERGIES	CROSS-SECTION	Err(mb)	PRECOMP(mb)	COMP(mb)	PACE
75.2	26.5	2.5	26.9	34.5	20.01
86.5	86.7	4.8	83	97.2	77.41
97.1	144.3	8	152	171	132
107	88.4	8.4	81.7	105	76.4
116.3	96.1	5.3	96	128	88
125.2	59.2	3.4	60.5	102	52.1
133.8	90.1	5	86.6	132	82.1
142.1	67.1	3.9	67.7	115	61
150.2	53.1	3.3	56.1	130	49.1

TAB5- 8: Theoretical and Measured cross-section for the reaction $^{59}_{27}\mathrm{Co}(^{20}_{10}\mathrm{Ne},\alpha 2\mathrm{pn})^{72}_{33}\mathrm{As}$

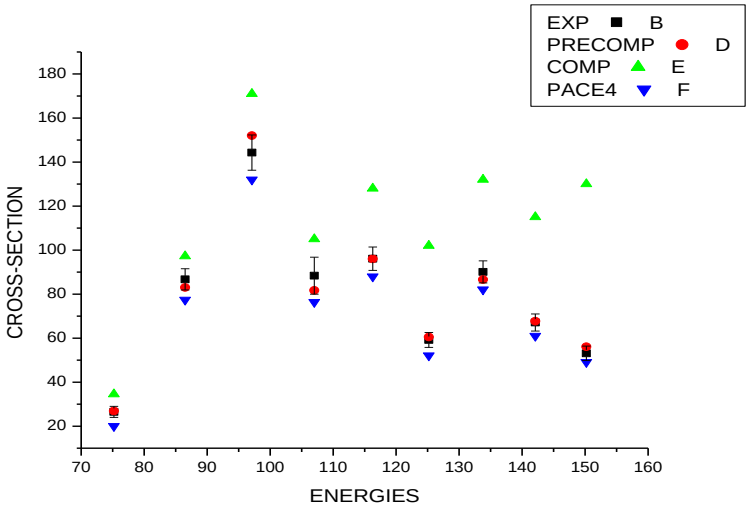

FIG5- 8: The production of Arsenic $^{59}_{27}\mathrm{Co}(^{20}_{10}\mathrm{Ne},2\mathrm{p}\alpha\mathrm{n})^{72}_{33}\mathrm{As}$

As shown in the graph above the theoretical cross sections calculated by PACE4 and complete, don't fit with the experimental cross sections at all projectile energies. So in this reaction the projectile is assumed to fuse with the target nucleus forming the excited state ^{79}Rb*, and this excited state emits two proton, one neutron and alpha, during the thermalization, leaving behind the residual nucleus $^{72}_{33}As$. Pre-equilibrium decay is seen in this reaction, while COMPLET-CN values are higher and PACE4 values are smaller.

$^{59}_{27}\mathrm{Co}(^{20}_{10}\mathrm{Ne}, 2\alpha)^{71}_{33}\mathrm{As}$

In the reaction $^{59}_{27}\mathrm{Co}(^{20}_{10}\mathrm{Ne}, 2\alpha)^{71}_{33}\mathrm{As}$ there is production of Arsenic $^{71}_{33}\mathrm{As}$ by emitting two alphas in the incident energies 75.2 -150.2Mev.

ENERGIES	σEXP(mb)	σErr(mb)	σCOMP(mb)	σ(mb)	σPACE(mb)
75.2	13.4	1	2.68E+00	2.00E+00	1.96E+00
86.5	59.4	7.8	1.15E+01	9.60E+00	1.03E+01
97.1	96.7	5.7	1.92E+01	1.45E+01	1.80E+01
107	131.9	9.4	2.48E+01	2.65E+01	1.86E+01
116.3	215.1	12.4	4.22E+01	3.20E+01	4.09E+01
125.2	179.8	10.5	3.50E+01	2.41E+01	3.30E+01
133.8	144.1	8.3	2.70E+01	1.95E+01	2.60E+01
142.1	126	7.4	2.53E+01	1.85E+01	2.49E+01
150.2	86.5	6.4	1.75E+01	1.42E+01	1.60E+01

TAB5- 9: Theoretical and Measured cross-section for the reaction $^{59}_{27}\mathrm{Co}(^{20}_{10}\mathrm{Ne}, 2\alpha)^{71}_{33}\mathrm{As}$

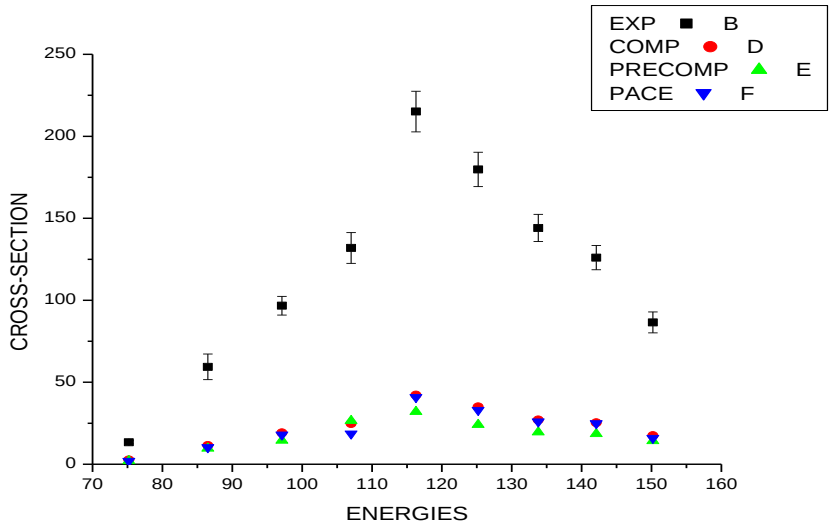

FIG5- 9: The production of Arsenic $^{59}_{27}\mathrm{Co}(^{20}_{10}\mathrm{Ne}, 2\alpha)^{71}_{33}\mathrm{As}$

As shown in the graph above, experimental results are much higher, at higher energies, than the theoretically calculated results using both codes. In this reaction the disagreement between the experimental and theoretical result can be resolved by assuming the incomplete fusion of ^{20}Ne in the cases of more alpha-particle emission (two alphas and three alphas) at higher energies. This shows incomplete fusion.

$^{59}_{27}\mathrm{Co}(^{20}_{10}\mathrm{Ne}, 2\alpha n)^{70}_{33}\mathrm{As}$

In the reaction $^{59}_{27}\mathrm{Co}(^{20}_{10}\mathrm{Ne}, 2\alpha n)^{70}_{33}\mathrm{As}$ there is production of Arsenic $^{70}_{33}\mathrm{As}$ by emitting two alphas and one neutron in the incident energies 62.9 -150.2MeV.

ENERGIES	σEXP(mb)	σErr(mb)	σCOMP(mb)	σPRECOMP(mb)	σPACE(mb)
62.9	22.5	2.5	1	4	2
75.2	44.7	4.7	3	11	1.23
86.5	63.7	4.4	2.2	5	3
97.1	62.9	3.7	6.12	4.36	6.55
107	77.6	3.8	4.11	3	4
116.3	162.7	7.1	7.8	12	7.85
125.2	213.5	8.6	12.3	5.33	2
133.8	246.2	8	9.36	2	3.66
142.1	118.1	3.9	7.12	7.92	8.23
150.2	58.5	2.4	0.999	1	3

TAB5- 10: Theoretical and Measured cross-section for the reaction $^{59}_{27}\mathrm{Co}(^{20}_{10}\mathrm{Ne}, 2\alpha n)^{70}_{33}\mathrm{As}$

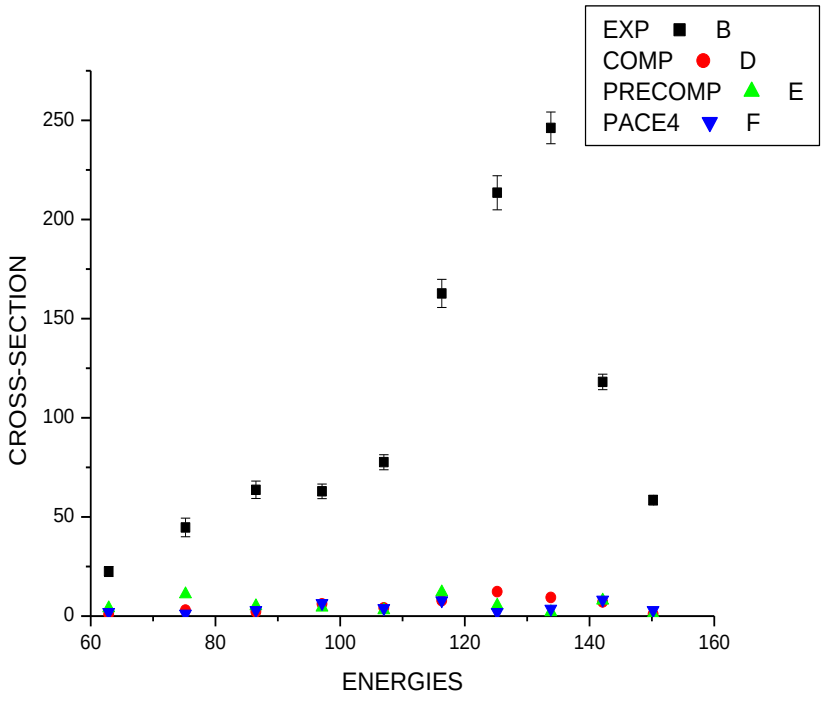

FIG5- 10: The production of Arsenic $^{59}_{27}\mathrm{Co}(^{20}_{10}\mathrm{Ne}, 2\alpha n)^{70}_{33}\mathrm{As}$

This is another example of emission of more than one alpha. The compound nucleus theory predicts negligible cross-section while experimental values are much higher. This reaction is again an example of incomplete fusion of projectile.

V.1.5.The production of GERMANIUM

$^{59}_{27}\mathrm{Co}(^{20}_{10}\mathrm{Ne}, 2\alpha\mathrm{pn})^{69}_{32}\mathrm{Ge}$

In the reaction $^{59}_{27}\mathrm{Co}(^{20}_{10}\mathrm{Ne}, 2\alpha\mathrm{pn})^{69}_{32}\mathrm{Ge}$ there is production of germanium $^{69}_{32}\mathrm{Ge}$ by emitting two alphas, one proton and one neutron in the incident energies 75.2 - 150.2Mev.

ENERGIES	σEXP(mb)	σErr(mb)	σCOMP(mb)	σPRECOMP(mb)	σPACE(mb)
97.1	107.7	4.3	1.00E+01	1.50E+01	2.00E+01
107	115.4	6.7	1.20E+01	1.32E+01	9.80E+00
116.3	146.7	5.8	4.25E+00	2.50E+00	1.03E+00
125.2	129	4.8	3.00E+00	2.00E-01	1.00E+00
133.8	120.6	4.8	8.60E+00	2.90E+00	7.45E+00
142.1	181.2	7.9	1.43E+01	5.00E+00	2.30E-01
150.2	160.1	7.8	5.00E+00	8.20E+00	2.00E+00

TAB5- 11: Theoretical and Measured cross-section for the reaction $^{59}_{27}\mathrm{Co}(^{20}_{10}\mathrm{Ne}, 2\alpha\mathrm{pn})^{69}_{32}\mathrm{Ge}$

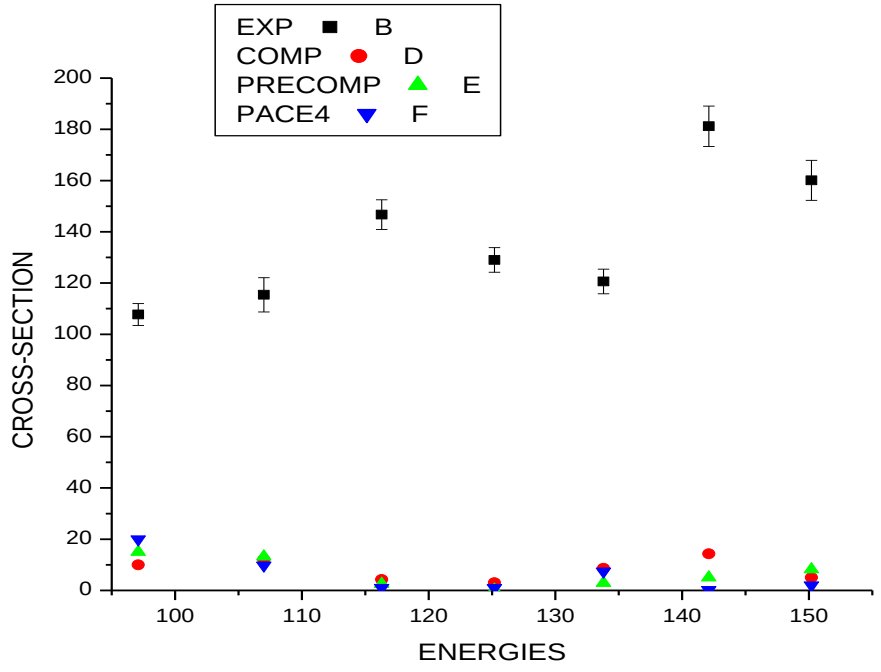

FIG5- 11: The production of Germanium $^{59}_{27}\mathrm{Co}(^{20}_{10}\mathrm{Ne}, 2\alpha\mathrm{pn})^{69}_{32}\mathrm{Ge}$

As shown in the graph above, two alphas are emitted so we have again incomplete fusion reaction.

V.1.6.The production of GALLIUM

$$^{59}_{27}\mathrm{Co}(^{20}_{10}\mathrm{Ne}, 3\alpha)^{67}_{31}\mathrm{Ga}$$

In the reaction $^{59}_{27}\mathrm{Co}(^{20}_{10}\mathrm{Ne}, 3\alpha)^{67}_{31}\mathrm{Ga}$there is production of gallium$^{67}_{31}\mathrm{Ga}$ by emitting three alphas in the incident energies 75.2 -150.2MeV.

ENERGIES	EXP(mb)	Err(mb)	COMP(mb)	PRECOMP(mb)	PACE(mb)
86.5	10.2	1.8	1.16E+01	1.06E+01	1.90E+01
97.1	23.1	3.1	2.44E+01	2.11E+01	3.16E+01
107	39.8	4.3	3.66E+01	2.95E+01	4.38E+01
116.3	118	5.5	5.41E+01	4.04E+01	5.59E+01
125.2	231.6	9.8	7.21E+01	4.93E+01	9.85E+01
133.8	271.2	12.3	1.01E+02	6.32E+01	1.24E+02
142.1	214	9.2	1.10E+02	6.20E+01	9.26E+01
150.2	327.7	15.2	1.14E+02	5.84E+01	1.15E+02

TAB5- 12: Theoretical and Measured cross-section for the reaction $^{59}_{27}\mathrm{Co}(^{20}_{10}\mathrm{Ne}, 3\alpha)^{67}_{31}\mathrm{Ga}$

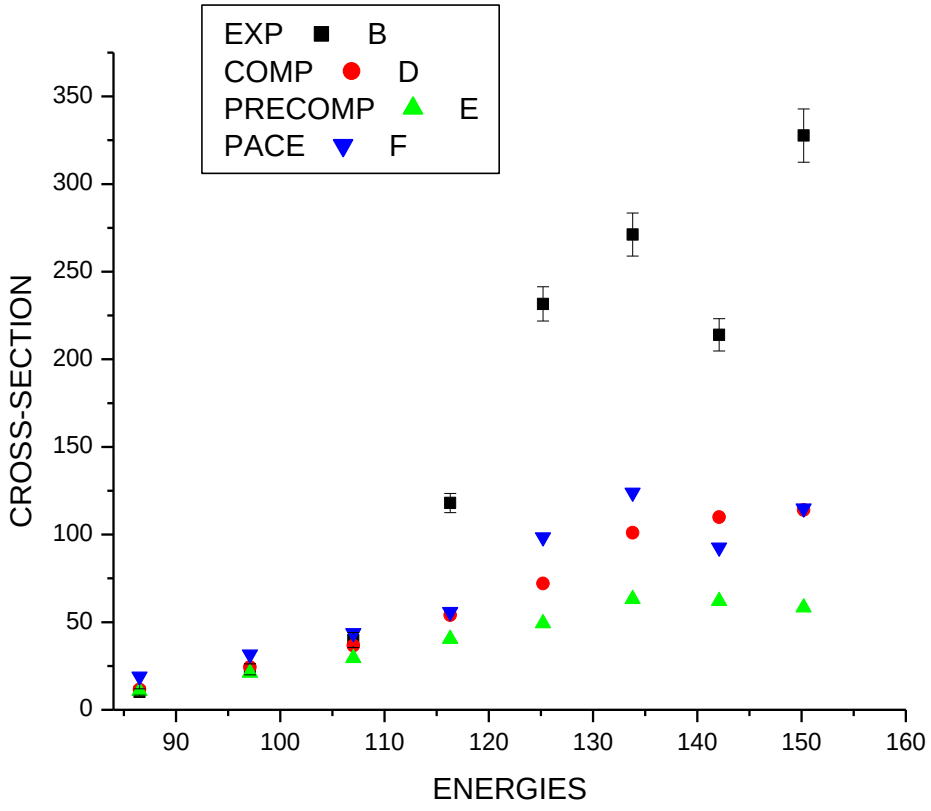

FIG5- 12: The production of Gallium $^{59}_{27}\mathrm{Co}(^{20}_{10}\mathrm{Ne}, 3\alpha)^{67}_{31}\mathrm{Ga}$

As clearly shown in figure above, for the $^{59}_{27}\mathrm{Co}(^{20}_{10}\mathrm{Ne}, 3\alpha)^{67}_{31}\mathrm{Ga}$, experimental results are much higher, at higher energies, than the theoretically calculated results using both codes. It is again a reaction explained on the basis of incomplete reaction fusion of the projectile. Only the measurement of energy spectrum of emitted particle may tell the type of the reaction.

$^{59}_{27}Co(^{20}_{10}Ne, 3\alpha n)^{66}_{31}Ga$

In the reaction $^{59}_{27}Co(^{20}_{10}Ne, 3\alpha n)^{66}_{31}Ga$there is production of gallium$^{66}_{31}Ga$ by emitting three alpha and neutron in the incident energies 86.5 -150.2Mev.

ENERGIES	EXP(mb)	Err(mb)	COMP(mb)	PRECOMP(mb)	PACE(mb)
86.5	112.7	8.3	5.94E+00	5.60E+00	6.012
97.1	88.1	6.4	2.69E+01	5.94E+00	27.8
107	120.4	12	4.39E+01	2.01E+00	44.13
116.3	108.1	7.6	5.33E+01	1.94E+00	54.9
125.2	125.1	12.5	5.73E+01	1.60E+01	50.3
133.8	161.9	16	4.31E+01	5.19E+01	44.98
142.1	232.8	23.1	4.15E+01	9.75E+01	43.87
150.2	261.7	26.7	4.25E+01	1.16E+02	43.56

TAB5- 13: Theoretical and Measured cross-section for the reaction $^{59}_{27}Co(^{20}_{10}Ne, 3\alpha n)^{66}_{31}Ga$

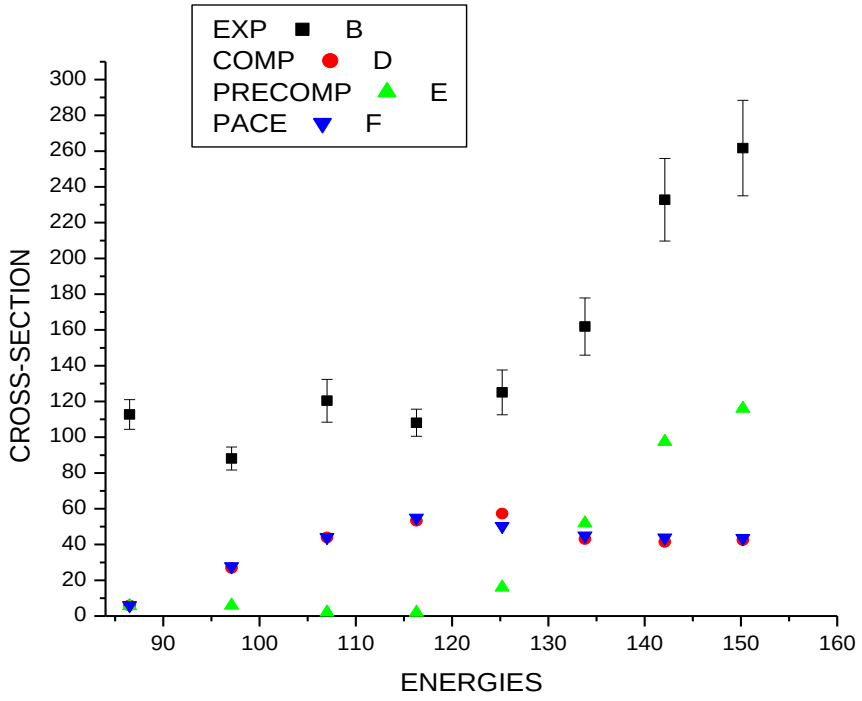

FIG5- 13: The production of Gallium $^{59}_{27}Co(^{20}_{10}Ne, 3\alpha n)^{66}_{31}Ga$

As clearly shown in figure above, for the$^{59}_{27}Co(^{20}_{10}Ne, 3\alpha n)^{66}_{31}Ga$, experimental results are much higher, at higher energies, than the theoretically calculated results using both codes. In this reaction the disagreement between the experimental and theoretical result can be resolved by assuming the incomplete fusion of ^{20}Ne .In the case of more alpha particles emission (two or three alpha) at higher energies. The

compound and pre-compound values are much smaller than experimental. This shows incomplete fusion.

V.1.7.The production of COPPER

$$^{59}_{27}\mathrm{Co}(^{20}_{10}\mathrm{Ne}, 4\alpha 2\mathrm{n})^{61}_{29}\mathrm{Cu}$$

In the reaction $^{59}_{27}\mathrm{Co}(^{20}_{10}\mathrm{Ne}, 4\alpha 2\mathrm{n})^{61}_{29}\mathrm{Cu}$there is production of copper$^{61}_{29}\mathrm{Cu}$ by emitting four alphas and two neutrons in the incident energies 97.1 -150.2Mev.

ENERGIES	EXP(mb)	Err(mb)	PACE
97.1	2.5	0.5	
107	18.4	3.6	1.23E-01
116.3	49.5	8	1.78
125.2	45.9	2.4	6.8
133.8	60.2	2.6	11.7
142.1	94.5	4.9	12.8
150.2	117.9	5	10.7

TAB5- 14: Theoretical and Measured cross-section for the reaction $^{59}_{27}\mathrm{Co}(^{20}_{10}\mathrm{Ne}, 4\alpha 2\mathrm{n})^{61}_{31}\mathrm{Cu}$

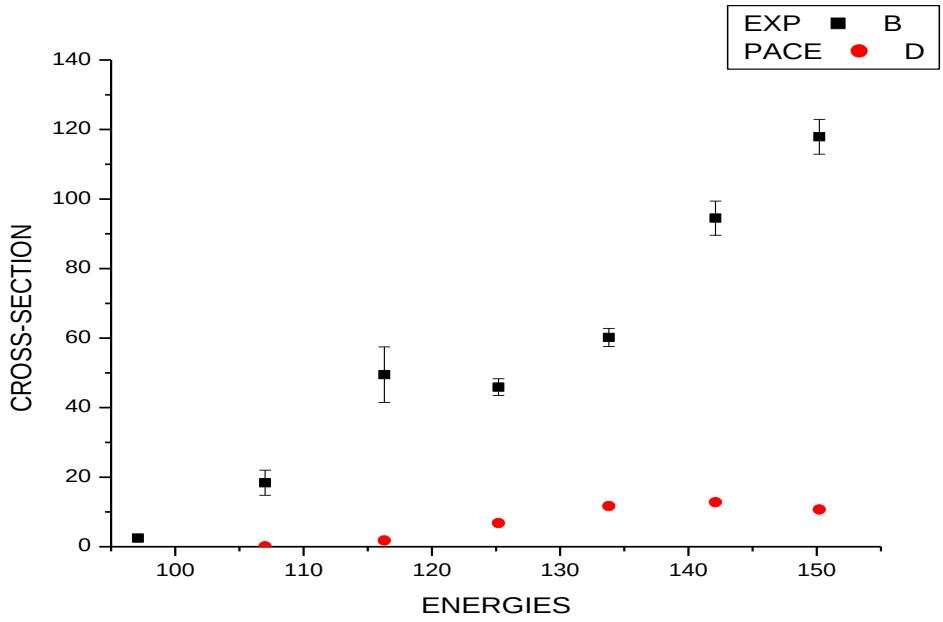

FIG5- 14: The production of Copper $^{59}_{27}\mathrm{Co}(^{20}_{10}\mathrm{Ne}, 4\alpha 2\mathrm{n})^{61}_{29}\mathrm{Cu}$

As clearly shown in figure above, for the$^{59}_{27}\mathrm{Co}(^{20}_{10}\mathrm{Ne}, 4\alpha 2\mathrm{n})^{61}_{29}\mathrm{Cu}$, experimental results are much higher, at higher energies, than the theoretically calculated results using PACE4 codes. This is again an example of emission of 4α at higher energies. The compound nucleus theory predicts almost negligible cross section while

experimental values are much higher .This reaction is again an example of incomplete fusion of projectile.

VI. CONCLUSION

Excitation functions for fourteen reactions in ^{20}Ne+^{59}Co system have been studied. The theoretical calculations based on PACE4 computer code and COMPLET computer code with a good choice of the parameters agrees well with the experimental data.

The experimental productions of cross-sections for non-alpha emitting channels are fitting with theoretical results which can be attributed to the complete fusion (CF) processes at those energies. This shows that the compound nucleus formation is seen.

The residues $^{77}_{36}$Kr ,$^{76}_{36}$Kr, $^{76}_{35}$Br ,were formed by complete fusion from excitation function $^{59}_{27}\mathrm{Co}(^{20}_{10}\mathrm{Ne},\mathrm{pn})^{77}_{36}\mathrm{Kr}$, $^{59}_{27}\mathrm{Co}(^{20}_{10}\mathrm{Ne},\mathrm{p2n})^{76}_{36}\mathrm{Kr}$, $^{59}_{27}\mathrm{Co}(^{20}_{10}\mathrm{Ne},\mathrm{2pn})^{76}_{35}\mathrm{Br}$ respectively.In this reaction the projectile fuse completely with the target nucleus forming the excited state ^{79}Rb*, and this excited state emits neutron and proton, etc.

In case of more than one alpha-emitting there are negligible productions of cross-sections, which may be attributed to incomplete fusion process at their relative energies.

The residues $^{71}_{33}$As , $^{70}_{33}$As ,$^{69}_{32}$Ge ,$^{67}_{31}$Ga ,$^{66}_{31}$Ga and $^{61}_{29}$Cu were formed by incomplete fusion processes from the excitation functions for the reactions : $^{59}_{27}\mathrm{Co}(^{20}_{10}\mathrm{Ne},2\alpha)^{71}_{33}\mathrm{As}$, $^{59}_{27}\mathrm{Co}(^{20}_{10}\mathrm{Ne},2\alpha\mathrm{n})^{70}_{33}\mathrm{As}$, $^{59}_{27}\mathrm{Co}(^{20}_{10}\mathrm{Ne},2\alpha\mathrm{pn})^{69}_{32}\mathrm{Ge}$, $^{59}_{27}\mathrm{Co}(^{20}_{10}\mathrm{Ne},3\alpha)^{67}_{31}\mathrm{Ga}$, $^{59}_{27}\mathrm{Co}(^{20}_{10}\mathrm{Ne},3\alpha\mathrm{n})^{66}_{31}\mathrm{Ga}$, $^{59}_{27}\mathrm{Co}(^{20}_{10}\mathrm{Ne},4\alpha2\mathrm{n})^{61}_{29}\mathrm{Cu}$ respectively. In this case a part of the projectile fuses with the target and rest of it is going into the beam direction with almost the same velocity as that of incident ion beam.

In the case of one alpha-emitting, the experimental productions of cross-sections for alpha-emitting channels are fitting with theoretical results which can attribute to the pre-compound reaction processes at those energies. This shows that the pre-compound nucleus formation is seen.

The residues $^{75}_{35}$Br , $^{74}_{35}$Br , $^{73}_{34}$Se , $^{70}_{34}$Se and $^{72}_{33}$As were formed by incomplete fusion processes from the excitation functions for the reactions: $^{59}_{27}\mathrm{Co}(^{20}_{10}\mathrm{Ne},\alpha)^{75}_{35}\mathrm{Br}$, $^{59}_{27}\mathrm{Co}(^{20}_{10}\mathrm{Ne},\alpha2\mathrm{n})^{74}_{35}\mathrm{Br}$, $^{59}_{27}\mathrm{Co}(^{20}_{10}\mathrm{Ne},\mathrm{p}\alpha\mathrm{n})^{73}_{34}\mathrm{Se}$, $^{59}_{27}\mathrm{Co}(^{20}_{10}\mathrm{Ne},\alpha\mathrm{p4n})^{70}_{34}\mathrm{Se}$, $^{59}_{27}\mathrm{Co}(^{20}_{10}\mathrm{Ne},2\mathrm{p}\alpha\mathrm{n})^{72}_{33}\mathrm{As}$ respectively.

REFERENCES

1. P.E.Hodgson, E.Gadioli and E.GadioliErba, Introductory Nuclear Physics,Oxford University Press, 2003.
2. Unnati, M.K.Sharma, B.P.Singh, S.Gupta, H.D.Bhardwaj, A.K.Sinha, International Journal of Modern Physics E, 2005.
3. M.K.Sharma, Unnati, B.K.Sharma, B.P.Singh, H.D.Bhardwaj, R.Kumar, K.S.Golda, and R.Prasad,Physical Review 70, 2004.
4. R. Prasad, D.P. Singh, A. Yadav, P.P.Singh, Unnati, M.K.Sharma, B.P.Singh, R.Kumar and K.S.Golda, ADS/P4-02, India.
5. Exfor library: http://www.nndc.bnl.gov/exfor.
6. J.Ernst, Institute for Solid State and Nuclear Physics, The Complet Code library: Complet.for; 445, Germany, 1997.
7. Walter E.Meyerhof, Elements of Nuclear Physics, McGraw-Hill,Inc, 1967.
8. B. Jean-Louis, R. James, S. Michel, Fundamentals in Nuclear Physics, Springer, 2004.
9. J.S.Lilley, Nuclear physics principles and Applications, John Wiley&Sons Ltd, 2001.
10. B. Bindu Kumar nad S. Mukherjee, Physical review C57, 1998.
11. C. Beck, F. A. Souza, N. Rowley, S. J. Sanders, N. Aissaoui, E. E. Alonso, P.Bednarczyk,N.Carlin,S. Courtin, A. Diaz-T , mm , , m, , , , , , , , , , , , , , A. Suaide, E. M.Szanto, A. Szanto de Toledo, S. Szilner, and J. Takahashi, Physical review C67, 2003.
12. K.F.Amanuel, PHD thesis, Addis Ababa University, Addis Ababa, Ethiopia, 2011.
13. A.F.Wudu,Master thesis, Addis Ababa University, Addis Ababa, Ethiopia, 2013.
14. BiniyamNigussie,Master thesis, Addis Ababa University, Addis Ababa, Ethiopia, 2012

DECLARATION

This thesis is my original work, has not been presented for a degree in any other University and that all the sources of material used for the thesis have been dully acknowledged.

Name: NTUMBA LOBO

Signature: _____

Place and time of submission: Addis Ababa University, June 2016

This thesis has been submitted for examination with my approval as University advisor.

Name: Prof.A.K. Chaubey

Signature: _____